Modeling, Analysis and Optimization of the Gas-Phase Methanol Synthesis Process

by

Abdulaziz Alarifi

A thesis
presented to the University of Waterloo
in fulfillment of the
thesis requirement for the degree of
Doctor of Philosophy
in
Chemical Engineering

Waterloo, Ontario, Canada, 2016

© Abdulaziz Alarifi 2016

AUTHOR'S DECLARATION

I hereby declare that I am the sole author of this thesis. This is a true copy of the thesis, including any required final revisions, as accepted by my examiners.

I understand that my thesis may be made electronically available to the public.

Abstract

Methanol synthesis has been the subject of many improvements over the last decades since it became more cost effective and scalable than earlier high pressure technology. The synthesis of methanol from syngas has conventionally been carried out in adiabatic quench-type reactor in the gas phase where the only way to moderate the temperature is to inject shots of syngas at various position of the rector. However, because of the highly exothermic behavior of methanol synthesis reactions, the dissipation of heat has been a bottle-neck in the reactor design, and reactor configurations have a tendency to be complicated.

This dissertation is divided into three parts presents a mathematical model of double-tube methanol reactor which was developed through cooperation between Mitsubishi Heavy Industries (MHI) and Mitsubishi Gas Company (MGC), methanol synthesis process flowsheet was developed and fully integrated with the Genetic Algorithms that generated a set of optimal operating conditions with respect to upper and lower limits and several constraints, and a dynamic optimization approaches to derive the ideal operating conditions for a Lurgi type reactor in the presence of catalyst deactivation.

The first part of dissertation concentrates on the Mitsubishi Methanol "superconverter" which has a design capability to efficiently remove the heat generated by the exothermic reactions in methanol synthesis and improves methanol production by at least 3% more than the conventional single-tube converter. This converter is operated under milder conditions, especially at the end of the reactor, allows the catalyst to last for a longer period. This leads to process intensification and allows for the use of a compact distillation step. In addition, this new design has the advantage of preheating the feed gas to the reactor by having the

inner tubes replace the feed gas preheater. The predicted methanol concentration and temperature profiles indicate that an increase in temperature is accompanied with a reduction in the methanol equilibrium concentration and hence limiting the profitability in the industrial plant. The use of a double-tube reactor is shown to be able to overcome this limitation. The novelty lies in a process modification which employs an inner tube that is disposed in the reactor and then the catalyst is charged into a circular space surrounded by the reaction tube on one side and inner tube on the other side. Simulation studies show that this design allows the temperature to increase gradually and, hence, delays the equilibrium to be reached to the end of the reactor. In other words, more methanol is produced and less byproducts.

The second part of the dissertation concentrates on a multi-objective optimization applied for the operating conditions of the methanol synthesis loop via a multi-stage fixed bed adiabatic reactor system with an additional inter-stage CO_2 quenching stream to maximize methanol production while reducing CO_2 emissions. The model prediction for the methanol synthesis loop at steady state showed good agreement against data from an existing commercial plant. Later, the process flowsheet was developed and fully integrated with the Genetic Algorithms Toolbox that generated a set of optimal operating conditions with respect to limits and linear constraints. The results showed methanol production was improved by injecting shots of carbon dioxide recovered from the reformer at various reactor locations.

The third part of the dissertation concentrates on a dynamic optimization approach derived the ideal operating conditions for a Lurgi-type methanol reactor in the presence of catalyst deactivation are proposed to determine the optimal use of recycle ratio of CO_2 and shell

coolant temperature without violating any process constraints. This study proposes a new approach based on a hybrid algorithm combining genetic algorithm (GA) and generalized pattern search (GPS) derivative-free methodologies to provide a sufficiently good solution to this dynamic optimization problem. The hybrid GA-GPS algorithm has the advantage of sequentially combining GA and GPS logics; while GA, as the most popular evolutionary algorithm, effectively explore the landscape of the fitness function and identify promising areas of the search space, GPS efficiently search existing basins in order to find an approximately optimal solution. The simulation results showed that implementing the shell temperature trajectory derived by the proposed approach with 5% recycle ratio of CO_2 increased the production of methanol by approximately 2.5% compared to the existing operating conditions.

Acknowledgements

I acknowledge, with gratitude, my debt of thanks to my supervisors, *Professor Ali Elkamel and Professor Eric Croiset,* for their warm encouragement and thoughtful guidance. I also want to express my deeply-felt thanks to the committee members of my dissertation, *Professor Ajay Ray, Professor Bill Anderson, Professor Zhongwei Chen, and Professor Fatih Erenay* for their insightful comments, and hard questions.

Table of Contents

List of Figures

List of Tables

Nomenclature

Parameters

$\Delta H_{r,j}$	Heat of reaction j, kJ/kmol.
a	Activity of catalyst.
A_c	Cross sectional area, m^2.
a_v	Specific surface area of catalyst pellet, $m^2\ m^{-3}$.
C_i, C_i^s	Concentration of component *i* in gas and catalyst surface, mol m^{-3}.
C_p , $c_{p,s}$	Heat capacity of gas mixture, kJ $kmol^{-1}\ K^{-1}$.
c_{p_g}	Heat capacity of gas mixture, kJ $kmol^{-1}\ K^{-1}$.
D_i	Internal diameter of tubes, m.
d_p	The particle diameter, m.
E_d	Activation energy used in the deactivation model, J mol^{-1}.
F_i	Molar flow rate of component *i* in fluid phase, mol/s.
F_{is}	Molar flow rate of component *i* in sold phase, mol/s.
G	Superficial mass velocity ($G=\rho_g\ u$), kg $m^{-2}\ s^{-1}$.
g_c	Conversion factor, equal one for the metric system.
h_f	Gas–solid heat transfer coefficient, W $m^{-2}\ K^{-1}$.
J	Total production, tonne.
$K_{ad,j}$	Adsorption equilibrium constant of component j.
K_d	Deactivation model parameter constant, s^{-1}.
$K_{eq,i}$	Equilibrium constant of reaction i.
k_{gi}	Mass transfer coefficient for component i ,m/ s.
k_i	Rate constant of reaction i.
L	Length of reactor, m.
MTBE	Methyl tert-butyl ether.
MTPD	Metric ton per day.
Mw_{MeOH}	Molecular weight of methanol, kg/kmol.
n_c	Number of components.

cont.

N_{eqs}	Number of equations.
N_c	Number of components.
N_{rxn}	Number of reaction.
N_{tubes}	Number of tubes.
N_{vars}	Number of variables.
P_j	Partial pressure of component j, bar.
r_{CH_3OH}	Rate of methanol synthesis reaction, kmol $hr^{-1}kg{\cdot}cat^{-1}$.
R_i	Rate of reaction for component i, mol kg^{-1} s^{-1}.
r_j	Rate of reaction j, mol kg^{-1} s^{-1}.
r_{RWGS}	Rate of water gas shift reaction, kmol hr^{-1} $kg{\cdot}cat^{-1}$.
R_T	Heat generated from all the reactions, kJ.
RWGS	The Reverse Water Gas Shift Reaction.
T	Gas phase temperature, K.
t	Time, s.
T_1, T_2, T_3	Temperature in tube 1 ,2 and 3, K.
T_R	Reference temperature, K.
T^s	Catalyst temperature, K.
T_{shell}	Shell coolant temperature, K.
T_w	Coolant temperature, K.
u	Gas velocity, m s^{-1}.
U_1, U_2	Overall heat transfer coefficient for tube 1 and 2, kW/m^2 K.
u_g	Gas velocity, m/s.
U_w	Overall heat transfer coefficient , kW/m^2 K.
u_z	Gas velocity in axial axis, m s^{-1}.
v	Volumetric flow rate, m^3/s.
$v_{i,j}$	Stoichiometric coefficient of component i in reaction j.
x	Dimensionless reactor length.
z	Reactor length, m.
$\varepsilon_b, \varepsilon_s$	Void fraction in catalyst bed and catalyst particle.

cont.

η_j	Effectiveness factor of reaction j.
μ_g	Viscosity of the gas mixture, kg s^{-1} m^{-1}.
ρ_b	Density of catalytic bed, kg/m^3.
ρ_f	Molar density of gas, mol m^{-3}.
ρ_g	Molar density of gas,mol/m^3
ρ_s	Density of catalyst, kg m^{-3}.
Φ	Void fraction of the bed (bed porosity).

Chapter 1: INTRODUCTION

METHANOL PRODUCTION AND USES

Methanol is the simplest alcohol that can be used as a building block to larger chemicals. It is a colorless polar liquid miscible with water at room temperature, highly toxic to humans and flammable nature. Special care must therefore be taken in handling, transportation and storage. The demand for cleaner and alternative energy is growing rapidly leading to interest in methanol production and increased of methanol demand is expected to potentially continue until the end of this decade. Methanol is extensively used as a raw material for formaldehyde production, MTBE and acetic acid.[1,2] In addition, methanol is also used in direct methanol fuel cell (DMFC), which is a subcategory of proton-exchange fuel cell in which methanol is used as fuel and directly oxidized with air to water and carbon dioxide while producing electricity.[3] Methanol is a suggested future clean fuel replacing fossil fuel as a means of energy storage, ground transportation fuel and raw material for its derivatives. It has been reported by U.S. Environmental Protection Agency (EPA) that switching gasoline to methanol would reduce 90% of the incidents caused by fuel.[4] Moreover, Methanol can be used as a diesel replacement which does not produce particulates or soot during combustion process.[5] It also burns at a lower temperature than diesel, consequently very low NOx emission is formed.[1,6]

Methanol was first produced by destructive distillation of wood in 1830. This process involves the pyrolysis of wood by heating to a high temperature in the absence or limited amounts of air and produces flammable liquid hydrocarbon mixtures including tar, terpenes, turpentine and methanol together with a solid residue of charcoal. Hence, it was commonly called wood alcohol or wood naphtha.

In 1923, Badische Anilin-und-Soda-Fabrik (BASF) introduced the first commercial-scale methanol manufacture process that used a zinc oxide / chromium oxide catalyst to convert carbon oxides and hydrogen into methanol at high pressure above 300 bar and temperature ranging from 350 to 400^{o}C. Major drawbacks for the high-pressure process are the high-energy consumption per ton of methanol and the imposed limitations on scaling potential.[7] After few decades, Imperial Chemical Industries (ICI) developed a low-pressure methanol process (LPM) in 1966 using copper/zinc based catalyst operating at lower pressures below 100 bar and temperatures between 200 to 300°C. The LPM eliminated much of capital and operating cost, and as a result, a global revolution in the way that methanol is produced.[8] Since that time, a typical methanol production plant requires three main steps:

- Syngas production
- Methanol synthesis
- Methanol purification/distillation

Syngas production

Synthesis gas or syngas is a mixture of carbon monoxide, carbon dioxide and hydrogen. Syngas can be produced from many sources, including natural gas, coal or petcoke and biomass.

Coal / Petcoke Gasification Process

Gasification is a high temperature process converts any carbon materials to synthesis gas. The feedstock typically is coal or petroleum coke, which reacts in the gasification with steam and oxygen at high temperature and high pressure.[9] The produced syngas must be treated to remove contaminates including sulfur, ammonia and small amount of hydrogen cyanide. Solid trace

elements associated with the feedstock such as mercury and arsenic are appeared in ash by-product. The major gasification reactions are listed in Table 1.1.

Table 1.1: Major Gasification Reactions.

Major reactions	Stoichiometric Equation
Gasification with oxygen	$C + 0.5\ O_2 \rightleftharpoons CO$ $C + \ O_2 \rightleftharpoons CO_2$
Gasification with Carbon Dioxide	$C + \ CO_2 \rightleftharpoons 2\ CO$
Gasification with Steam	$C + \ H_2O \rightleftharpoons CO + H_2$
Gasification with Hydrogen	$C + 2H_2 \rightleftharpoons CH_4$
Water-Gas Shift	$CO + H_2O \rightleftharpoons H_2 + CO_2$
Methanation	$CO + 3H_2 \rightleftharpoons \ CH_4 + H_2O$

The feedstock is grounded and mixed with water to form slurry and then pumped into the gasifier and mixed with oxygen at high temperature to produce synthesis gas with a H_2/CO ratio is 0.6. Water-gas shift converter is used to adjust the ratio to 2.

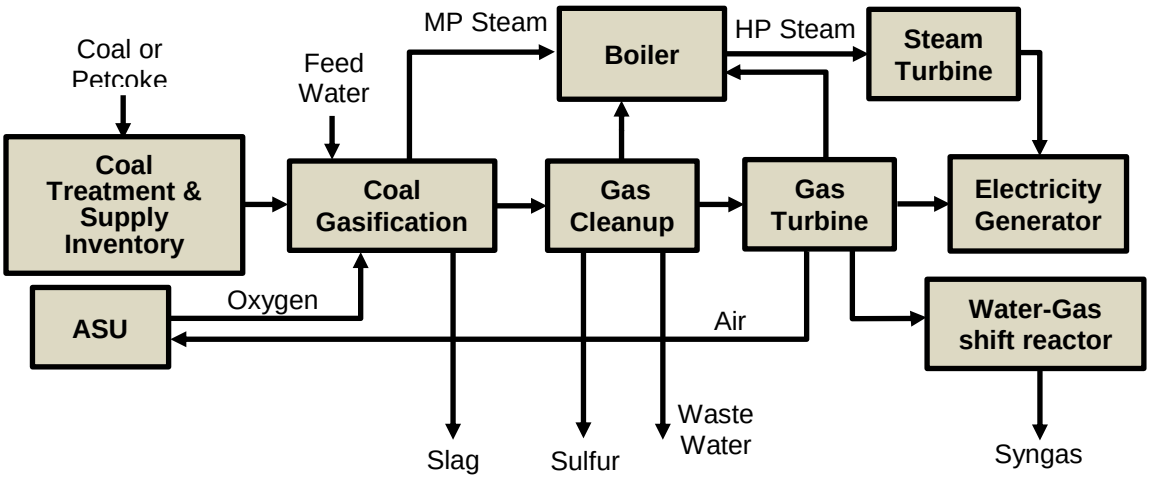

Figure 1.1: Gasification Block diagram.

The general flow scheme of gasification process shows in Figure 1.1, as illustrated, the medium pressure steam leaving the gasification is heated by the boiler to generate power.

Natural Gas based Process

Synthesis gas can be formed via partial oxidation (POX), steam reforming of natural gas (SMR) and autothermal reforming (ATR). A desulfurization unit may be used prior to the introduction into syngas production process in order to remove any sulfur species in natural gas and to prevent rapid catalyst deactivation. In POX process, natural gas reacts with pure oxygen in a flame chamber at high temperature of 1,200-1,500^{o}C. The POX process typically produces syngas with hydrogen and carbon monoxide ratio (H_2/CO) of below 2. The SMR process consists of two major parts, a packed catalyst in tubes and a furnace to heat the reformer tubes.[10] The feed of reformer tubes is a mixture of desulfurized natural gas and steam with required steam to carbon ratio (S/C) of 3:1 to suppress the coke formation on a nickel catalyst at 800-1000 ^{o}C and to boost the rate of water-shift reactions toward more a hydrogen rich syngas (H_2/O_2) above 3:1. Figure 1.2 illustrates the block diagram of conventional steam methane reforming process.

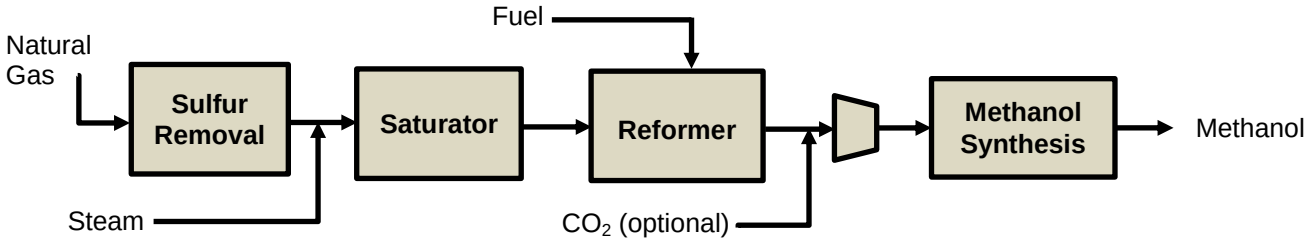

Figure 1.2: Block Diagram of Conventional Steam Methane Reforming process.

ATR process concept incorporates the benefits of combining POX and SMR. The advantage of ATR reformer is the self-heating by the partial oxidation of methane takes place in a single chamber, and consequently reducing capital cost because the system is simpler than SMR and produced a desired H_2/CO ratio of slightly higher than 2.1. The summary of autothermal reforming reactions is listed in Table 1.2.

Table 1.2: major autothermal reforming reactions.[11]

Major reactions	Stoichiometric Equation
Partial oxidation of methane	$CH_4 + 0.5\ O_2 \rightarrow CO + 2H_2$
Steam reforming	$CH_4 + H_2O \longrightarrow CO + 3H_2$
Water-gas shift	$CO + H_2O \rightleftharpoons CO_2 + H_2$
coke formation	$2CO(g) \longrightarrow CO_2(g) + C(s)$

Methanol synthesis

The conversion of syngas into methanol is an exothermic process. Thus, its thermal behavior must be clearly understood to select the suitable reactor design, operation procedure and catalyst performance. Methanol is typically synthesized in gas phase over Cu/ZnO based catalyst through hydrogenation of carbon monoxide and carbon dioxide:[7]

$$CO + 2\ H_2 \leftrightarrow CH_3OH \qquad \Delta H^o_{298} = -21.7\ \text{kcal/mol} \qquad (1.1)$$

$$CO_2 + 3\ H_2 \leftrightarrow CH_3OH + H_2O \qquad \Delta H^o_{298} = -11.9\ \text{kcal/mol} \qquad (1.2)$$

Both exothermic reactions (1.1) and (1.2) are simultaneously occurred and exhibit a contraction in volume. Therefore, methanol synthesis is favored at high pressure and low temperature. A reverse water-gas shift reaction (1.3) is also occurred over the catalyst toward CO production.

$$CO_2 + H_2 \leftrightarrow CO + H_2O \qquad \Delta H^o_{298} = 9.8\ \text{kcal/mol} \qquad (1.3)$$

As mentioned above, Imperial Chemical Industries (ICI) introduced the first LPM process, which is based on $Cu/ZnO/Al_2O_3$ catalyst, operates under much lower pressure and milder temperature than high pressure ZnO/Cr_2O_3 catalyst. The copper based catalyst is very active and selective toward methanol. However, it is particularly sensitive to sulfur species. Many authors have

intensively studied the kinetics of methanol synthesis. Natta derived the first kinetic model for ZnO/Cr_2O_3 catalyst of high pressure. It was developed based on the assumption that the rate limiting step is the reaction of carbon monoxide and two of hydrogen molecules in the adsorption status.[12] As listed in Table 1.2, this model ignored any influence of CO_2 presence and its constants were empirically evaluated for each type of catalyst. Later, Bakemeier et al. observed the contradiction between their experiments of CO_2 rich feeds and Natta's predictions.[13] Thus, CO_2 influence was introduced in the rate equation as a Langmuir adsorbate molecule and assumed desorption of methanol from the catalyst surface is the rate limited step in the mechanism. Leonov et al. proposed the earliest kinetic model for the low-pressure $Cu/ZnO/Al_2O_3$ catalyst and similar to Natta's model for high pressure chrome based catalyst, there is no CO_2-dependent term presented in the rate equation.[14] Klier et al. considered the effects of CO_2 on methanol synthesis rate over the low pressure copper based catalyst by conducting many experiments at $CO_2/CO/H_2$ ratios between 0/30/70 and 30/0/70. It was found that the methanol conversion rate increases substantially with the addition of CO_2, up to 10%, and at higher concentration of CO_2, the strong adsorption of CO_2 would physically cover active sites on the catalyst and leads to rapid catalyst deactivation.[15,16] Graaf et al. assumed that methanol can be formed from three independent reactions namely CO and CO_2 hydrogenation as well as the reverse water-gas shift reaction.[17] For their studies, a commercial $Cu/ZnO/Al_2O_3$ catalyst was tested in a spinning basket reactor at pressure ranged between 15-50 bar and temperature between 201-245^{o}C. The suggested kinetic model was based on the assumption that a dual-site adsorption mechanism accurately describes the sequence of molecular reactions steps take place on the catalyst surface. McNeil et al. generated new kinetics data for methanol synthesis over $Cu/ZnO/Al_2O_3$ and proposed a rate

expression for methanol synthesis based on the mechanistic assumptions that hydrogen adsorption only occurs on ZnO active sites.[18] They concluded that, as reported by Klier et al., CO_2 is strongly absorbed on Cu^{1+} and inhibits methanol production rate. As result, an overall rate expression includes the influence of both CO_2 and CO. Unlike Graaf el al. kinetic model, Froment and Bussche developed a new kinetic model effectively couples both the overall methanol synthesis rate and the reverse water-gas shift reaction.[19] Their experiments were conducted on an industrial $Cu/ZnO/Al_2O_3$ catalyst filled in an integral reactor after being ground and diluted with an inert for the sake of minimizing the effect of internal mass and heat transfer of the catalyst and maintaining the operating temperature fixed along the reactor. As reported, this model includes the effect of inlet temperature, pressure and gas compositions and capable to accurately predict both reaction outside the experimental ranges. Among the kinetic models for low pressure methanol synthesis in gas phase over $Cu/ZnO/Al_2O_3$ catalyst, the kinetic model developed by Vanden Bussche and Froment appeared to be suitable for predicting the experimental data from an industrial reactor scale. The kinetic models mentioned above a long with their operating conditions are listed in Table 1.3.

Table 1.3: kinetic model of methanol synthesis as reported by several authors

Researchers	Rate expressions	Operating condition
Natta et al., 1955	$r_{CH_3OH} = \dfrac{\gamma_{CO} p_{CO} \left(\gamma_{H_2} p_{H_2}\right)^2 - \dfrac{\gamma_{CH_3OH}\, p_{CH_3OH}}{K_{eq1}}}{\left(A + B\,\gamma_{CO}\, p_{CO} + C\,\gamma_{H_2} p_{H_2} + D\,\gamma_{CH_3OH}\, p_{CH_3OH}\right)^3}$	200-250 atm 300-360 ^{o}C
Leonov et al., 1973	$r_{CH_3OH} = k\left(\dfrac{p_{CO}^{0.5} p_{H_2}}{p_{CH_3OH}^{0.66}} - \dfrac{p_{CH_3OH}^{0.34}}{p_{CO}^{0.5} p_{H_2} K_2^*}\right)$	493-533 K; 40-55 atm
Klier et al.,1982	$r_{CH_3OH} = const\ \dfrac{K_{redox}^3 \left(\dfrac{p_{CO_2}}{p_{CO}}\right)^3 \left(p_{CO}\, p_{H_2}^2 - \dfrac{p_{CH_3OH}}{K_2^*}\right)}{\left[1 + K_{redox}\left(\dfrac{p_{CO_2}}{p_{CO}}\right)\right]^3 \left(F + K_{CO_2}\, p_{CO_2}\right)^n} + k'\left(p_{CO_2} - (1/K_1^*)\left(p_{CH_3OH}\, p_{H_2O}/p_{H_2}^3\right)\right)$	225 - 250°C 75 atm
Graaf et al., 1988	$r_1 = \dfrac{k_1 K_{CO}\left[f_{CO} f_{H_2}^{3/2} - \dfrac{f_{CH_3OH}}{f_{H_2}^{1/2} K_{p_1}^o}\right]}{\left(1 + K_{CO} f_{CO} + K_{CO_2} f_{CO_2}\right)\left[f_{H_2}^{1/2} + \left(K_{H_2O}/K_{H_2}^{1/2}\right) f_{H_2O}\right]}$ $r_2 = \dfrac{k_2 K_{CO_2}\left(f_{CO_2} f_{H_2} - \dfrac{f_{H_2O} f_{CO}}{K_{p_2}^o}\right)}{\left(1 + K_{CO} f_{CO} + K_{CO_2} f_{CO_2}\right)\left[f_{H_2}^{1/2} + \left(K_{H_2O}/K_{H_2}^{1/2}\right) f_{H_2O}\right]}$ $r_3 = \dfrac{k_3 K_{CO_2}\left[f_{CO_2} f_{H_2}^{3/2} - \dfrac{f_{CH_3OH} f_{H_2O}}{f_{H_2}^{3/2} K_{p_3}^o}\right]}{\left(1 + K_{CO} f_{CO} + K_{CO_2} f_{CO_2}\right)\left[f_{H_2}^{1/2} + \left(K_{H_2O}/K_{H_2}^{1/2}\right) f_{H_2O}\right]}$	483-518 K 15-50 bar
McNeil et al., 1989	$r_{MeOH} = \dfrac{k_f' K_{CH} K_{H_2}^2 K_H^2 K_{CO}\left(p_{CO} p_{H_2}^2 - p_{CH_3OH}/K_{eq}\right)}{K_{CH} K_{H_2}^{3/2} K_H^{3/2} K_{CO} p_{CO} p_{H_2}^{3/2} + K_{CO_2} p_{CO_2} + K_{H_2}' p_{H_2}} + \dfrac{k_f'' K_{H_2} K_H\, K_{CO_2} K_{CHO_2}\left[p_{CO_2} p_{H_2} - p_{CH_3OH}\, p_{H_2O}/\left(K_{eq}'' p_{H_2}^2\right)\right]}{K_{H_2}^{1/2} K_H^{1/2} K_{CO_2} K_{CHO_2} p_{CO_2} p_{H_2}^{1/2} + K_{CO_2}'' p_{CO_2}^2 + K_{H_2O}\, p_{H_2O}^3}$	483-513K 2.89-4.38 MPa
Froment et al.,1996	$r_{MeOH} = \dfrac{k_{5a}'\, K_2'\, K_3\, K_4\, K_{H_2}\, p_{CO_2}\, p_{H_2}\left[1 - (1/K^*)\left(p_{H_2O}\, p_{CH_3OH}/p_{H_2}^3\, p_{CO_2}\right)\right]}{\left(1 + \left(K_{H_2O}/K_8\, K_9\, K_{H_2}\right)\left(p_{H_2O}/p_{H_2}\right) + \sqrt{K_{H_2}\, p_{H_2}} + K_{H_2O}\, p_{H_2O}\right)^3}$ $r_{RWGS} = \dfrac{k_1' p_{CO_2}\left[1 - K_3^*\left(p_{H_2O}\, p_{CO}/p_{CO_2}\, p_{H_2}\right)\right]}{\left(1 + \left(K_{H_2O}/K_8\, K_9\, K_{H_2}\right)\left(p_{H_2O}/p_{H_2}\right) + \sqrt{K_{H_2}\, p_{H_2}} + K_{H_2O}\, p_{H_2O}\right)}$	453-553 K 15-51 bar

Methanol process technologies are fairly standard since ICI introduced the first low pressure methanol (LPM) process in 1960s. The LPM revolutionized the industry of methanol, and, as result the methanol production increased rapidly over the world. Several licensers now offer complete methanol plants, starting from either coal or natural gas as feedstock. The catalysts are almost the same composed of copper and zinc oxides over alumina oxide support. The main differences in these processes are mainly in the design of the reactor itself and in the way of integrating units for more economical and/or profitable operation. The ideal synthesis gas stoichiometry also called the stoichiometric number, defined by this formula $(H_2–CO_2)/(CO+CO_2) = 2\text{-}2.1$, as CO_2 is involved in the reverse gas-water shift reaction.

The ICI low-pressure methanol synthesis process was made possible after because the desulfurization of the syngas became more efficient to reduce sulfur components to be less than 0.5 ppm. Producing sulfur free syngas enables LPM process to be existed, resulted in a significant reduction of compression duty in the recycle loop and lower temperature witch improved the selectivity of methanol over by-products of light organic components.

The incoming natural gas feed to the reformer is pre-heated in desulfurization preheater using heat from the reformer waste heat duct and then passed to hydrogenation catalyst, where any organic sulfur compounds such as COS and SO_2 are converted to H_2S and finally removed by passing the gas through either one or two zinc oxide beds.[20] Amine gas treating, also known as amine-scrubbing MDEA can be used for bulk desulfurization and CO_2 capturing of syngas from coal gasification or petcoke containing several thousand of ppm of sulfur and excess amount of carbon dioxide. Water-gas shift converter can also be further used to adjust syngas ratio.

ICI low pressure methanol synthesis reactor consists of a single vessel filled by catalyst in stages and quench cooled by lozenge distributors placed between stages.[21] This design permits a good gas distribution and mixing as well as easy loading and unloading of catalyst. A schematic diagram of quench adiabatic reactor is shown in Figure 1.3, the temperature profile of this reactor type is known to be extremely high at the end of each stage.

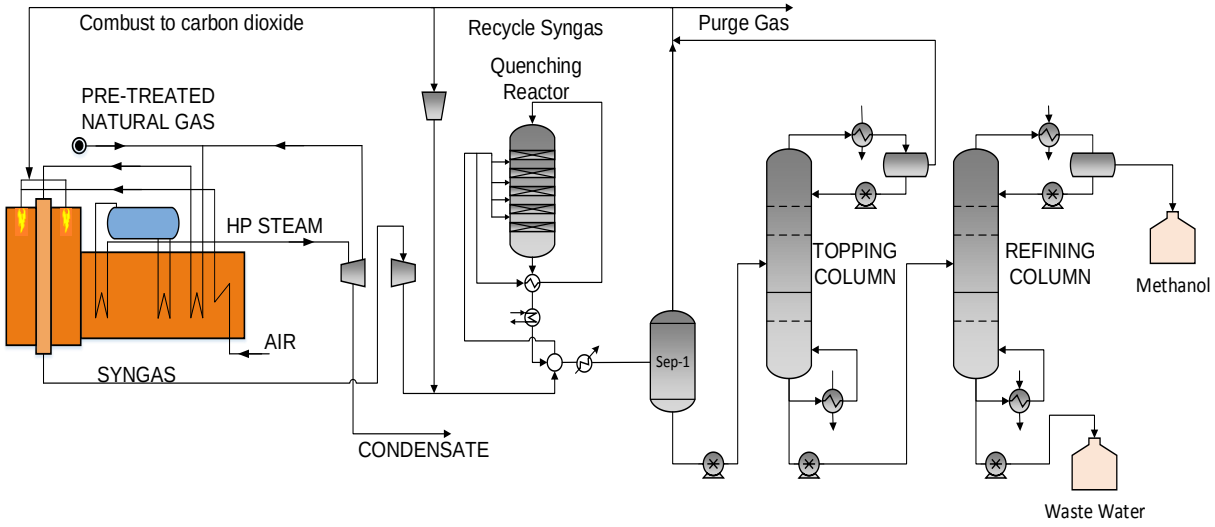

Figure 1.3: ICI low pressure methanol process flow diagram.

As shown in Figure 1.3, the syngas is compressed to 50 atm in a centrifugal compressor and fed into a quench adiabatic converter. The product gas from the adiabatic reactor is then cooled and the crude methanol condensed. The crude methanol contains, beside methanol and water, a number of organic chemicals synthesized at the same time as methanol. The concentration of theses impurities is low and consists of dimethyl ether, methyl ester, some paraffinic hydrocarbons, ethanol and higher alcohols, and other complexes. The purge gas or not condensable gas stream is recycled to the reformer furnace for use as fuel. The converter design must assure the inlet gas is uniformly distributed to prevent rapid local overheating spots that may

cause sintering and rapid deactivation of the catalyst. Thermal stability of the reactor is of utmost important characteristics in designing a new converter. A good reactor design allows an easy procedure of handling, loading and unloading catalyst in reactor as well as servicing and maintaining reactors and vessels. Consequently, startup and shutdown time is greatly reduced.

In the process offers by Lurgi, a tubular packed-bed converter is operated at temperature between 250 to 260 ^{o}C and pressure between 50 to 60 bar. The Lurgi reactor design consists of shell and tubes where the tubes are packed with catalyst and the heat of reaction is removed by circulating coolant water on the shell side. In contrast to quench adiabatic reactor, the tubular reactor is a relatively complex design. However, it is one of the most efficient systems, as the heat is directly removed to generate medium pressure steam. For an operational point of view, Lurgi reactor type has some advantages, such as the temperature profile is almost isothermal with low a temperature drop not more than 10-12^{o}C along the tube, and thus high selectivity obtained. This thermal stability leads to a smaller amount of catalyst required compared with quench adiabatic reactor. This type of reactor is relatively insensitive to the feed temperature change and directly controlled via shell coolant temperature.

Mitsubishi Gas Chemical Company (MGC) and Mitsubishi Heavy Industries, Ltd. (MHI) developed a low pressure methanol synthesis process based on double-tube type vertical heat exchanger design, it is so called “superconverter”.[22] A diagram of superconverter design is shown in Figure 1.4, the catalyst is packed in the annual space of the tube and the boiler water circulates in the shell side. MGC/MHI stated that this new type of reactor has the rate of the one-pass reaction increased, and it is excellent at recovering the heat of reactions.

■ **ICI quench adiabatic converter**

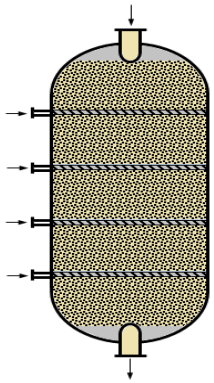

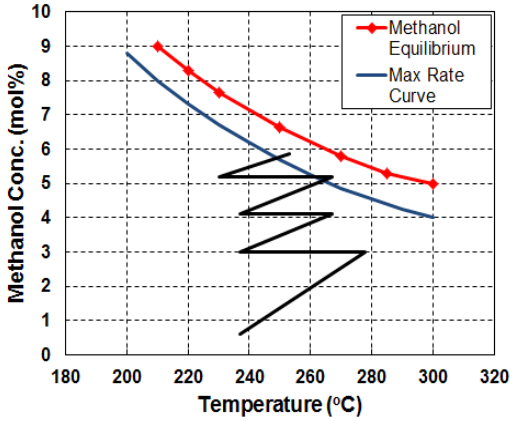

■ **Lurgi converter**

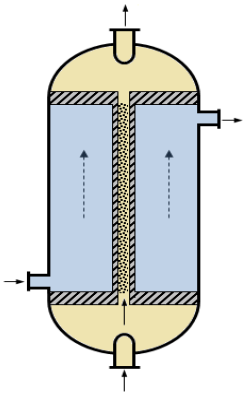

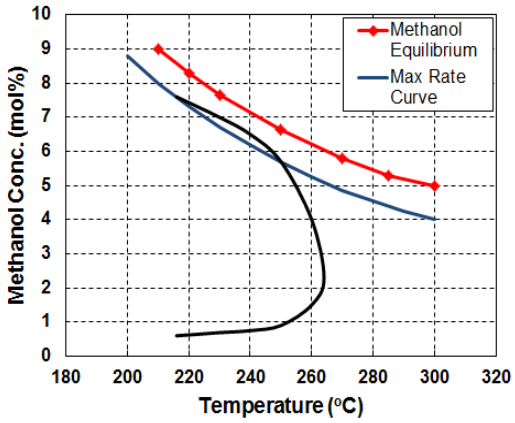

■ **Mitsubishi superconverter**

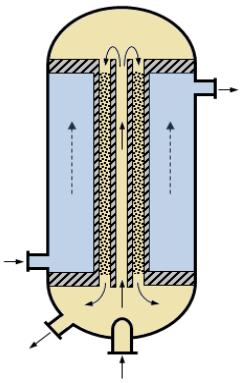

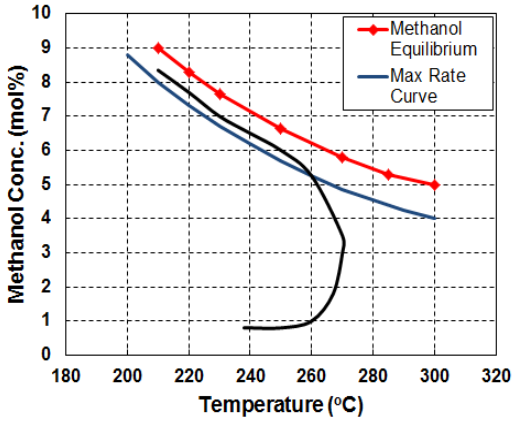

Figure 1.4:Three main methanol synthesis converters.

The inlet gases flow first through the inner tubes from the bottom toward the top and in the meantime preheat it by the heat of reactions take place in the annular side. After reaching the top

of the vessel, gas flows through the catalyst bed in the opposite direction from the top to the bottom, both gases in inner and annular tube are counter-current to ensure a good heat transfer between two sides. The temperature profile in the annular side is favorable in terms of reaction rate and conversion.

Methanol purification/distillation

There are two U.S Federal Grades of methanol, Grade AA and Grade A. the methanol minimum weight percentage of Grade AA and Grade A are the same 99.85% whereas water maximum weight are 0.1% and 0.15% respectively.[20] Typically grade A of crude methanol requires two distillation columns, whereas Grade AA requires three distillation columns. The first distillation column operates at elevated pressure and the second column operates at atmospheric pressure.

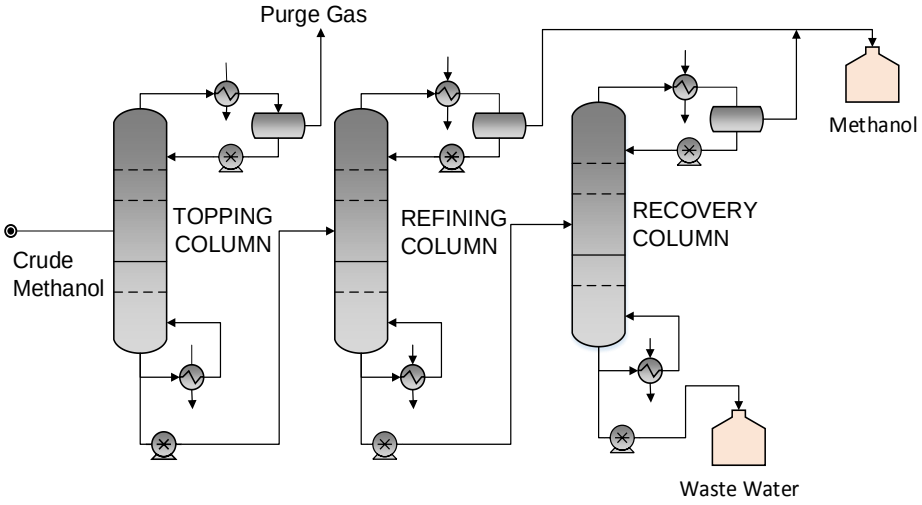

Figure 1.5: Three columns methanol distillation system (Grade AA).

Mitsubishi Gas Chemical (MGC) has an advantage of ongoing development to the methanol process including environmental improvement by introducing additional equipment such as humidifier, after the distillation system, which result decrease in generation of waste water while

reduce the amount of boiler water. The steam containing unreacted (hydrogen, carbon monoxide and carbon dioxide) is then recycled to the reformer and the syngas compression section. A good understating of both reactor and the synthesis reactions is needed to propose the optimal operation police. This policy can be adjusted while the catalyst is deactivated to maintain constant methanol production rate.

SCOPE OF THE THESIS

This thesis deals primarily with optimization and modeling of gas-phase methanol synthesis process. At the stage of modeling, attention is focused on constructing rigorous and reliable models for various types of reactors, describing accurately the complex chemical and physical phenomena take place inside the system and their interaction. These sets of nonlinear partial differential equations are solved with respect to the reactor length, and later on, discretized by means of method of lines to account for catalyst deactivation. This make the system formulated mathematically as dynamic optimization problem with continuous variables that provides a scalar quantitative performance measure that needs to be optimized. The optimization techniques for solving derivative-free optimization problem and finding optimum operating conditions are given a great attention. The main emphasis of this thesis is to provide an improvement in methanol production, aiming at addressing the following:

- Comparative study between Single- and Double- tube industrial reactors for methanol synthesis process.
- Simulation and multi-objective optimization of a methanol synthesis process using quench adiabatic reactor, prospective on methanol production and CO_2 utilization.

- Demonstrate the effectiveness and robustness of derivative-free search algorithm-based methods on industrial-scale cases.
- Describe and analysis a hybrid metaheuristics algorithm which was implemented to rapidly find the optimum operating conditions for methanol synthesis process with undergoing catalyst deactivation.

OUTLINE OF THE THESIS

This thesis is written and organized in the form of manuscript-based thesis. Chapters 2 and 3 have been published in peer reviewed journals. Chapter 4 has been accepted for potential publication.

Chapter 1 gives an introduction to methanol uses, synthesis process and various types of industrial reactors.

Chapter 2 presents the mathematical model of double-tube reactor and its design features to enhance methanol production.

Chapter 3 deals with methanol synthesis process flowsheet that was developed and fully integrated with the Genetic Algorithms Toolbox that generated a set of optimal operating conditions with respect to upper and lower limits and several constraints. The optimization of methanol synthesis has been carried out with the elitist non-dominated sorting genetic algorithm (NSGA-II).

Chapter 4 presents mathematical model for industrial Lurgi-type methanol reactor with catalyst deactivation optimized with respect to the shell coolant temperature and the recycle ratio of CO_2 fed to the system. Hybrid algorithm combining genetic algorithm (GA) and generalized pattern search (GPS) was used to provide sufficiently good solution and converge faster than GA alone.

Chapter 5 delivers an overall conclusion for the thesis & recommendations for future work.

Chapter 2: Steady State Simulation of a Novel Annular Multitubular Reactor for Enhanced Methanol Production

ABSTRACT

In this study, a one-dimensional heterogeneous model with intraparticle diffusion limitation has been developed for methanol synthesis from syngas. The synthesis gas produced from the reformer is compressed at a pressure of 60−100 bar and then heated up to 200−250 °C in order to prepare it for methanol production reactions. Syngas reacts on a copper oxide/zinc oxide/alumina catalyst. The annular multitubular (AMT) reactor proposed in this article has a design capability to efficiently remove the heat generated by the exothermic reactions in methanol synthesis and improves methanol production by at least 3% more than the conventional converter. In addition, the converter is operated under milder conditions, especially at the end of the tube, which makes the catalyst last for a longer period. This leads to process intensification and allows for the use of a compact distillation step. In addition, this new design has the advantage of preheating the feed gas in the reaction by having the inner tubes replace the feed gas preheater. Methanol production and temperature profile are the most important characteristics of methanol synthesis reactor. The predicted methanol concentration and temperature profile indicate that an increase in temperature is accompanied with a reduction in the methanol equilibrium concentration and hence limits profitability in the industrial plant. The use of an AMT reactor is shown to be able to overcome this limitation. The novelty lies in a process modification that employs an inner tube that is disposed in the reactor and then the catalyst is charged into a circular space surrounded by the reaction tube on one side and inner tube on the other side. Simulation studies show that this

design allows the temperature to increase gradually, and hence, delays the equilibrium so as to reach the end of the reactor. In other words, more methanol is produced and less byproducts.

INTRODUCTION

The demand for methanol has been growing at an average annual rate of 10% since 2010, and this increase is expected to potentially continue until the end of this decade. Methanol is mainly used as a raw material for formaldehyde production, accounting for almost 27% of the world's consumption. The use of methanol as direct fuel is the second-largest market at almost 11%, with acetic acid as the third-largest type of methanol end use. China is the largest consumer, comprising almost 41% of universal consumption.[20] Recently, there has been a movement toward employing methanol to replace hydrogen as a fuel for the future, since it is easy to store and can be readily used in the current infrastructure of fuel stations; this is not the case with hydrogen.[23] As a result, many organizations have redirected their research focus. For example, the U.S Department of Energy decided to stop funding hydrogen gas production and storage research from 2010 onward.[24] Methanol can be easily transformed to dimethyl ether (DME) or directly to olefins, which makes it potentially in more demand.[25] Methanol technologies are licensed by numerous companies such as Davy Process Technology (DPT) and Johnson Matthey Catalyst (JM), Lurgi, Mitsubishi Gas Chemical (MGC), and Haldor Topsoe. Methanol technologies consist of two major stages.[26] The first stage is the generation of synthesis gas (carbon oxides and hydrogen) from reforming natural gas (methane) or other heavy hydrocarbon feedstock such as crude oil, naphtha, or coal. Synthesis gas from reforming or gasifying processes is characterized by a stoichiometric number, $SN= (H_2 - CO_2)/(CO + CO_2)$. The second stage is the production of

methanol from the synthesis gas. The current low-pressure processes operating at 50−100 bar in the vapor phase is widely used to produce methanol from synthesis gas.

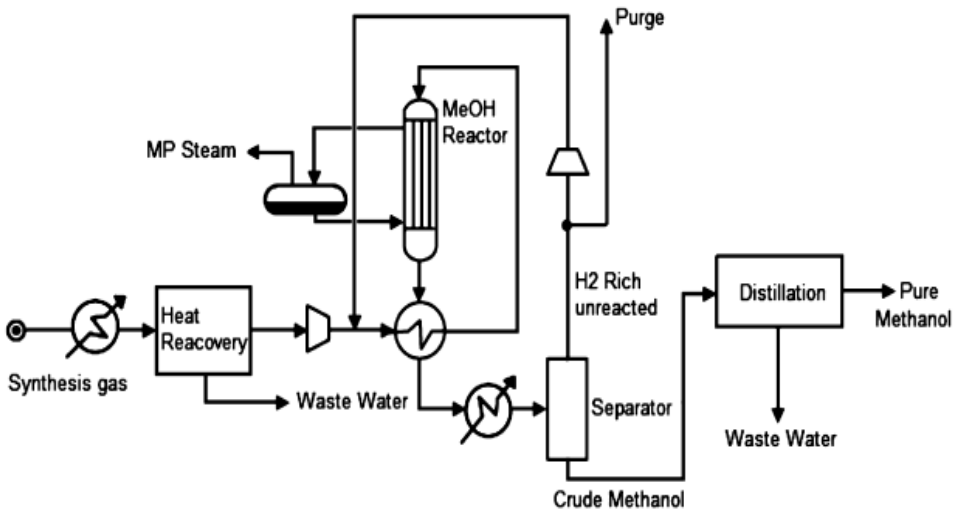

Figure 2.1: Process flow diagram of methanol synthesis.

The flow diagram is illustrated in Figure 2.1, where the converter is either a tubular heat exchanger (Lurgi), a double-tube heat exchanger (Mitsubishi) superconverter, or a multiple stage adiabatic quenching reactor (methanol Casale) and is normally used for plants requiring no steam in the synthesis unit, However, it is a low-cost reactor. The superconverter was developed and is owned by MGC and Mitsubishi Heavy Industrial (MHI); it consists of a simple converter with a double tubular heat exchanger, where the catalyst is packed in the shell side, between the inner tube and outer tube, as shown in Figure 2.2.

As reflected in the potential demand for methanol, many new plants have been built across the world, especially in the Middle East. In the first quarter of 2008, a new mega methanol plant (Ar-Razi No. 5) began on stream, with an annual capacity of 1.7 million tons. This plant is located in Jubail, Saudi Arabia and is owned by SABIC and a Japanese consortium led by Mitsubishi.

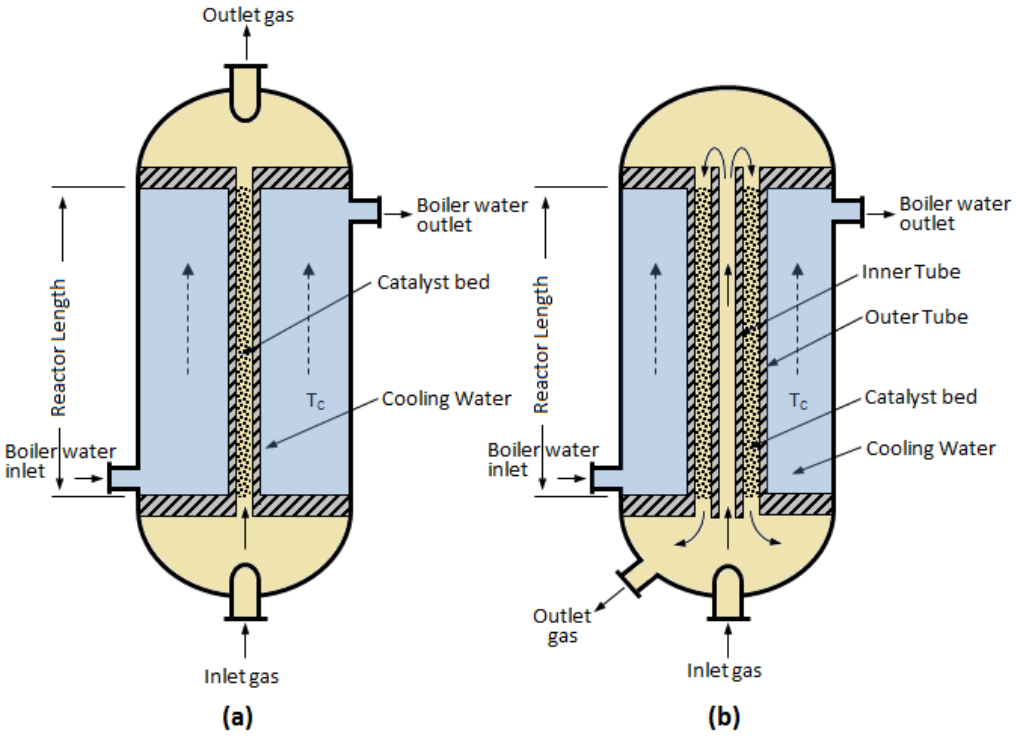

Figure 2.2: Schematic configuration of (a) a conventional tubular reactor and (b) a double tube reactor.

Moreover, in 2012, the Qatar Fuel Additives Company awarded a contract to MHI to build a new methanol plant with a capacity of 1 million tons per year. MGC and MHI own and patented a new methanol process including the additional humidifiers coming after the distillations, which result in a smaller amount of wasted water released to the environment while reducing the amount of water fed into the boiler.[27] In addition, they improved the performance of the converter by inventing a superconverter, which is basically a simple tubular heat exchanger where the catalyst is filled in the annular side, between inner and outer tubes. This configuration provides a methanol process in which the distillation system is reduced in size by efficiently removing the heat generated by the reactions and inhibits byproducts.

MODEL DEVELOPMENT

Reaction Kinetics

Many researchers have studied the kinetics of methanol synthesis. Three main reactions may possibly occur, namely: (i) hydrogenation of carbon monoxide to methanol (2.1), (ii) hydrogenation of carbon dioxide to methanol (2.2), and (iii) a reverse water gas shift reaction (2.3).

$$CO + 2H_2 \rightleftharpoons CH_3OH \quad (2.1)$$

$$CO_2 + 3H_2 \rightleftharpoons CH_3OH + H_2O \quad (2.2)$$

$$CO_2 + H_2 \rightleftharpoons CO + H_2O \quad (2.3)$$

Early kinetic models were derived for the ZnO/Cr_2O_3 catalyst of high-pressure processes, which has been now almost completely abandoned in favor of low-pressure technology.[12,28] Leonov et al. were the first to model methanol synthesis kinetics over a $Cu/ZnO/Al_2O_3$ catalyst.[14] Their model again assumed CO to be the source of carbon in methanol and did not account for the influence of CO_2 in the feed. Klier et al.[16] considered other components as sources of carbon, but assumed that CO is the most important source of carbon in methanol. Later, McNeil et al.[18] expanded on the mechanism of the direct hydrogenation of CO_2 and the possible role of ZnO as a hydrogen reservoir. Despite the much larger number of parameters in the resulting model, the latter authors did not manage to show a significantly better agreement between the experimental and the simulated results than that already obtained by Klier et al.[16] Villa et al.[29] realized that a thorough modeling of the methanol synthesis system should also involve a description of the water-gas shift reaction. Graaf et al.[30,31,17] considered both hydrogenation of CO and CO_2 as well as a water-gas shift reaction. Parallel to these developments, Russian groups led by Rozovskii and Temkin[32]

developed several kinetic models for the $Cu/ZnO/Al_2O_3$ catalysts. Since neither of these groups ever succeeded in producing methanol from a dry mixture of CO and hydrogen, the models are all based on the direct hydrogenation of CO_2 to methanol, while a majority also account for the occurrence of a water-gas shift reaction. The present view is that methanol is formed from CO_2 over a copper-containing catalyst. This is confirmed by C-14 labeling[33,34] and in situ measurements.[35] The kinetic model proposed by Vanden Bussche and Froment[19] for the conversion of syngas over $Cu/ZnO/Al_2O_3$ catalyst accurately predicts the kinetic behavior reported from other authors outside the experimental window and kinetic equations describe the influence of inlet temperature, pressure, and feed composition in a physically acceptable way. In this work, we have adopted the Vanden Bussche and Froment kinetic model.

The main rate expressions and equilibrium relation are as follows:

$$r_{CH_3OH} = \frac{k_1 P_{CO_2} P_{H_2} \left[1 - \frac{1}{K_{eq1}} \frac{P_{H_2O}\, P_{CH_3OH}}{P_{H_2}^3\, P_{CO_2}}\right]}{(1 + K_{ad1} \frac{P_{H_2O}}{P_{H_2}} + K_{ad2}\, P_{H_2}^{0.5} + K_{ad3}\, P_{H_2O})^3} \qquad (2.4)$$

$$r_{RWGS} = \frac{k_2\, P_{CO_2} \left[1 - K_{eq2} \frac{P_{H_2O}\, P_{CO}}{P_{H_2}\, P_{CO_2}}\right]}{\left[1 + K_{ad1}\, \frac{P_{H_2O}}{P_{H_2}} + K_{ad2}\, P_{H_2}^{0.5} + K_{ad3}\, P_{H_2O}\right]} \qquad (2.5)$$

Equilibrium relations:

$$log_{10}(K_{eq1}) = \frac{3066}{T} - 10.592 \qquad (2.6)$$

$$log_{10}(K_{eq2}) = -\frac{2073}{T} + 2.029 \qquad (2.7)$$

The reaction rate and adsorption constants are of the Arrhenius form, with constants as given below in Table 2.1.

Table 2.1: reactions rates and adsorptions parameters.

$k_i = A_i\ exp\left(\frac{B_i}{RT}\right)$	A	B
k_1	1.07	-36696
k_2	11.22×10^{10}	94765
k_{ad1}	3453.38	
k_{ad2}	0.499	17197
k_{ad3}	6.62×10^{-11}	124199

Heterogeneous Model

A one-dimensional heterogeneous model with intraparticle diffusion limitation has been developed for an annular multitubular (AMT) reactor. This model accounts for a double tube heat exchanger that is employed to remove the heat generated by the methanol synthesis exothermic reactions. This new synthesis reactor is a simple double-tube type vertical exchanger. The catalyst is packed in the annular space and the boiler water circulates in the shell side (see Figure 2.2b). The feed gas first flows into the inner tube from the bottom toward the top and is preheated by heat generated in the catalyst bed that is then collected at the top of the reactor and flows into the catalyst bed. The catalyst bed is cooled by the boiling water circulating in the shell side and the feed gas preheated in the inner tube. The mass and energy balances for the fluid phase are:

$$u_z \frac{\partial C_i}{\partial z} = k_{g,i} a_v (C_i^s - C_i) \tag{2.8}$$

$$u_z \rho_f c_p \frac{\partial T_2}{\partial z} = h_f\ a_v (T^s - T_2) + \frac{\pi D_2 U_{w2}}{A_{c_2}} (T_{shell} - T_2) + \frac{\pi D_1 U_{w1}}{A_{c_1}} (T_1 - T_2) \tag{2.9}$$

where C_i is the concentration of component i and T_2 is the temperature inside the shell side. The solid-phase equations are expressed by:

$$\rho_b \sum_{j=1}^{N_{rxn}} v_{ij} r_j(C_i^s, T^s) = -k_{g,i} a_v (C_i^s - C_i) \quad (2.10)$$

$$\rho_b \sum_{j=1}^{N_{rxn}} r_j(C_i^s, T^s) \left(-\Delta H_{r,j}(T^s)\right) = h_f a_v (T^s - T_2) \quad (2.11)$$

The inner tube is disposed in the reaction tube to preheat the reactants while they flow upward to the top of the reactor. The tube side (feed reactants gas flow) energy balance is

$$u_z \rho_f c_p \frac{\partial T1}{\partial z} = -\frac{\pi D_1}{A c_1} (T_1 - T_2) \quad (2.12)$$

T_1 is the temperature of the reactants when they flow through the tube. The Ergun equation has been used to predict the pressure drop along the shell side of the reactor with the following boundary conditions:

$$\frac{dp}{dz} = -\frac{G}{\rho\, g_c\, d_p} \left(\frac{1-\phi}{\phi^3}\right) \left[\frac{150(1-\phi)\mu}{d_p} + 1.75\, G\right] \quad (2.13)$$

$C_i(0)=C_{i,0}$, $T_2(0)=T_{2,0}$

$T_1(1)=T_{1,0}$, $P(0)=P_0$.

Dusty-Gas Model for Diffusion Limitation in Porous Catalyst

The following sets of differential equations are the mass balances of each component along the pellet radius:

$$\frac{D_e^i}{10^{-5} R_g T_s R_p^2} \left(\frac{d^2 p_s^i}{d\xi^2} + \frac{2}{\xi} \frac{dp_s^i}{d\xi}\right) + \rho_s \sum_{j=1}^{N_{rxn}} v_{ij} r_j = 0 \quad (2.14)$$

where $\xi = r/r_p$ and the boundary conditions are as follows:

$$\left.\frac{dp_s^i}{d\xi}\right|_{\xi=0} = 0 \;\; i = 1 \ldots\ldots n_c \quad (2.15)$$

$$-D_e^i \left.\frac{dp_s^i}{d\xi}\right|_{\xi=1} = k_g^i \left(p_s^i|_{\xi=1} - p_{bulk}^i\right) \;\; i = 1 \ldots . n_c \quad (2.16)$$

Hence, the effectiveness factor is calculated by using this formula:

$$\eta_j = \frac{3\int_0^1 r_j \xi^2 d\xi}{r_j^s} \qquad (2.17)$$

Figure 2.3 shows the effectiveness factor along the dimensionless reactor length. The diffusion and heat-transfer correlations are listed in Table 2.2.

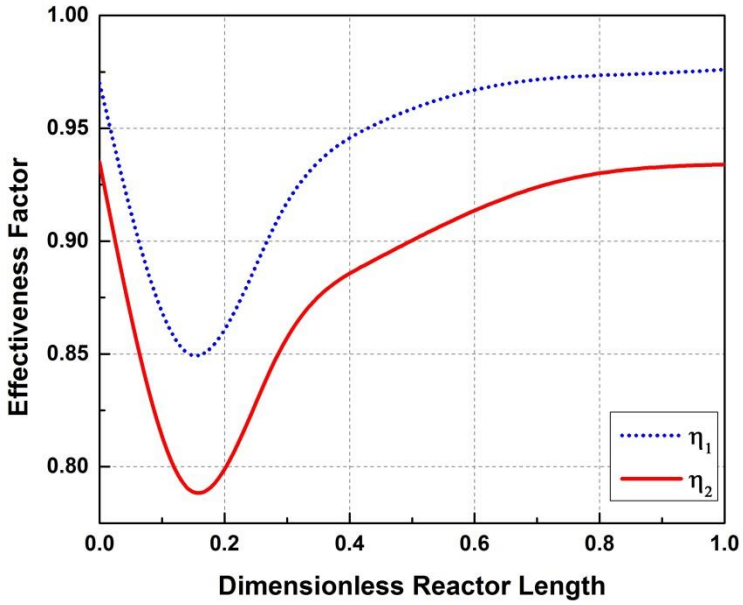

Figure 2.3: Effectiveness factor obtained for reaction rate r_{MeOH} and r_{RWSDS} along the dimensionless reactor length.

Computational Techniques

Differential and nonlinear algebraic equations of the reactor model (2.8)-(2.13) were numerically solved by Matlab Gear's method stiff solver ode15s. This solver uses backward differentiation formulas (BDFs) simultaneously, using fsolve for the set of nonlinear solid phase equations. Emden's equations generated by the dusty-gas model were solved by Matlab boundary value problem solver bvp4c by identifying the singular terms 2/ξ in the program.

Table 2.2: Diffusion and heat transfer parameters.

Parameter	source	Mathematical Expression
Effective and Kudsen diffusion coefficients	Ref 36	$D_e^i = \frac{\varepsilon_s}{\tau}\left(\frac{1}{D_m^i} + \frac{1}{D_k^i}\right)$
		$D_K^i = R_{pore}\frac{4}{3}\left(\frac{2}{\pi}\frac{R_g T}{Mw^i}\right)^{1/2}$
Multicomponent molecular diffusion coefficient	Ref 37	$D_m^i = \sum_{j=1}^{n_c, j\neq i} \frac{y_s^j}{D_b^{ij}}$
Binary diffusion coefficient	Refs 38-40	$D_b^{ij} = \frac{0.143\, T^{1.75}}{P_s\, W_m^{0.5}\left(V_i^{1/3} + V_j^{1/3}\right)^2}$
		$W_m^{ij} = \frac{2}{\frac{1}{Mw^i} + \frac{1}{Mw^j}}$
Mass transfer coefficient	Ref 41	$k_g^i = 1.17 \times 10^3 Re^{-0.42} Sc^{i^{-0.67}} u_g$
		$Sc^i = \frac{\mu}{\rho_g D_m^i \times 10^{-4}}$
		$Re = \frac{2R_p u_g}{\mu}$
Overall heat transfer coefficients	Ref 42	$\frac{1}{U_w} = \frac{1}{h_w} + \frac{d_t}{6\,\lambda_{er}}\frac{Bi+3}{Bi+4}$
Nusselt number	Refs 43 and 44	$Nu_w = \frac{h_w d_{pv}}{\lambda_f}$ $= \frac{8\,\beta_s}{d_t/d_{pv}}, Re > 50$ $= \frac{8\,\beta_s}{d_t/d_{pv}} + 2\,Bi_s\frac{\lambda_{rs}}{\lambda_f}\frac{d_{pv}}{d_t}\left(1 + \frac{\beta_f}{\lambda_{rs}/\lambda_f}\right),$
Biot number (Dixon 2007).	Ref 45	$Bi^{-1} = Bi_f^{-1} + Bi_s^{-1}$
		$Bi_f = Nu_{fw}\left(\frac{d_t}{2\,d_{pv}}\right)\left(\frac{Pe_{rf}}{Re\,Pr}\right)$
		$Bi_s = 0.48 + 0.192\left(\frac{d_t}{d_{pv}} - 1\right)^2$

RESULTS AND DISCUSSION

Model validation was carried out by comparing the model results with the process data provided by a new 10 t/d pilot plant reactor constructed at MGC's Niigata Plant.[46] Design and catalyst specifications are summarized in Table 2.3.

Table 2.3: Design and Catalyst Specifications of a 10 t/d Pilot Plant Constructed at MGC's Niigata Plant.

Parameter	Value
Catalyst tube length	20 m
Outer tube diameter	85 mm o.d., 75 mm i.d.
Inner tube diameter	19 mm o.d., 17 mm i.d.
Number of catalyst tubes	6
Tubes material	carbon - 0.5% Mo
Shell material	carbon steel
Capacity	10 t/d
Pressure range	45-110 kg/cm^2
Catalyst type	Cu /ZnO/Al_2O_3
$\rho_s(kg\ m^{-3})$	1214
$d_p(m)$	6.53×10^{-3}
$\lambda_s(W\ m^{-1}k^{-1})$	0.004
$a_v(m^{-1})$	626.98
ε_s/τ	0.123

The pilot plant used for this study has six catalyst tubes arranged circumferentially in the reactor, each with a length of 20 m, for the purpose of imposing severe conditions and predicting the behavior of a comparable longitudinal size used in the commercial plant.

Methanol production and temperature profile are the most important characteristics of methanol synthesis reactor.

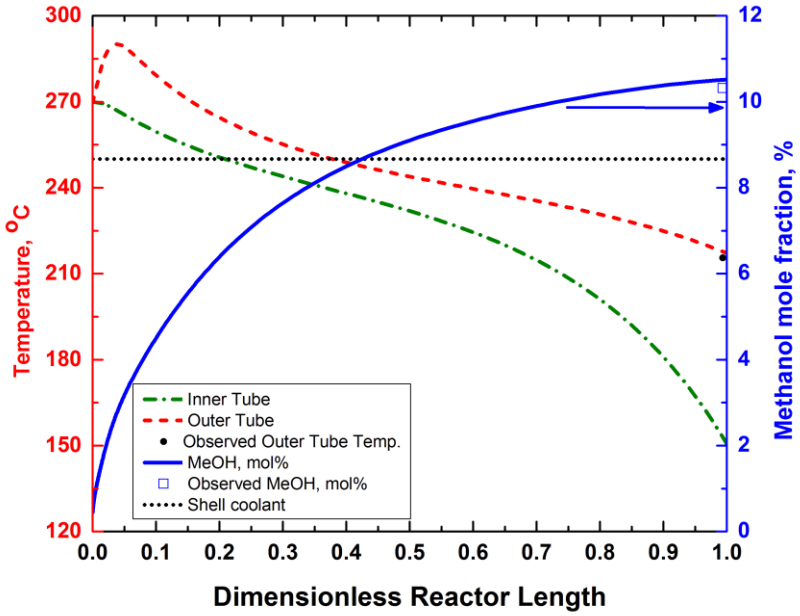

Figure 2.4: Temperature profile and methanol mole percentage versus pilot plant operation for double tube reactor.

The predicted results for methanol concentration and temperature profile with the corresponding observed data are shown in Figure 2.4. The gas temperature peaks at one meter near the catalyst tube inlet and then decreases while flowing toward the outlet. The observed reactor performance agrees well with the model results as presented in Table 2.4.

A comparison study was performed in order to assess the performance of the new reactor versus the conventional tubular reactor. The latter reactor is comprised of a tube (packed with catalyst) that is externally cooled by boiler water and a nearly isothermal temperature profile is formed in the catalyst bed and aims at recovering to the maximum possible extent the heat of the synthesis reaction in the form of high-pressure steam.

Table 2.4: Experimental and simulation results of pilot plant using a new methanol synthesis reactor.

Parameter	Inlet	Outlet	
		Observed	Calculated
Compositions (mol%)			
CH_3OH	0.39	10.32	10.51
CO_2	5.78	5.39	5.25
CO	8.93	2.37	1.97
H_2O	0.09	1.64	1.25
H_2	72.06	65.01	64.48
N_2	0.69	0.83	1.34
CH_4	12.06	14.44	15.2
Space Velocity (h^{-1})	6260		
Cooling Temp (^oC)	250		
Temperature (^oC)	150	215.5	217.17
Pressure (bar)	62.3	55	56.14

The tube equivalent diameter of a conventional reactor was calculated to give a similar cross-sectional area of the new reactor; both reactors have an identical amount of catalyst and have similar operating conditions. This comparison was conducted under the conditions presented in Table 2.5.

Table 2.5: Inlet compositions and operation conditions.

Parameter	**Gas A**	**Gas B**
Compositions (mol%)		
CH_3OH	0	0
CO_2	8	5
CO	9	8
H_2O	0	0
H_2	65	80
N_2	5	1
CH_4	13	6
Space Velocity (h^{-1})	3000-6000	
Cooling Temp. (^oC)	250	
Feed Temp. (^oC)	150	
Pressure (bar)	59-98	

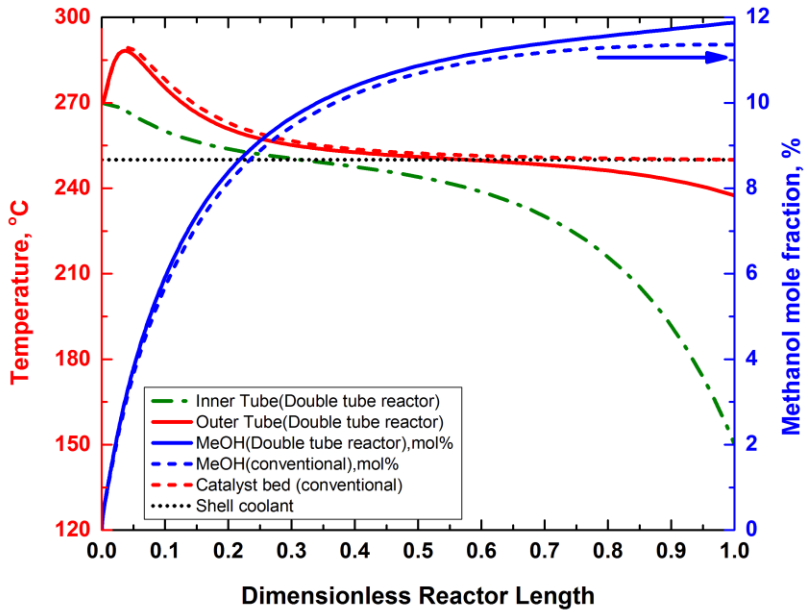

Figure 2.5: Comparison of MeOH % and temperature profile along the reactor length between new reactor and conventional reactor (P=98 bar and SV=6000 h^{-1}).

Figure 2.5 shows the temperature profiles of a conventional reactor and a double tube reactor; both are identical before reaching the peak temperature and then the conventional reactor temperature gradually decreases to reach the cooling temperature bottom line, whereas the new reactor still undergoes a decreasing temperature profile toward the outlet.

This latter temperature profile is very favorable in terms of reaction rate, and encourages the production of methanol. The methanol mole fraction profile increases gradually and reaches 11.36% and 11.92% for the double tube exchanger and the conventional converter, respectively. Hence, the production of methanol is improved by ~3%, compared to the conventional converter, while at the same time the converter is operated under mild conditions, especially at the end of the tube, which makes the catalyst last longer. Furthermore, a one-dimensional analysis was carried out for two different cases of feed gas composition. The first case is a typical syngas composition

produced via the combination of steam reforming and partial oxidation for natural gas reformer (gas A), and the other case is a syngas produced via steam reforming of natural gas (gas B). For different gas compositions, the case of rich hydrogen content (gas B) shows a sharper temperature peak at the inlet stage of the catalyst tube than the lower hydrogen content gas (gas A), as shown in Figure 2.6. The methanol concentration profiles are almost identical, except that gas A is higher than gas B at the outlet, since it has more carbon oxides and its SN ratio is closer to the optimal value. Figure 2.7 shows the model results of different synthesis pressures ranging from 59 bar up to 98 bar. Higher synthesis pressures lead to an increase of reaction rate, but the removal of reaction heat becomes more difficult. Based on Le Chatelier's Principle, the production of methanol can be improved by increasing the synthesis pressure, and this is consistent with the current results.

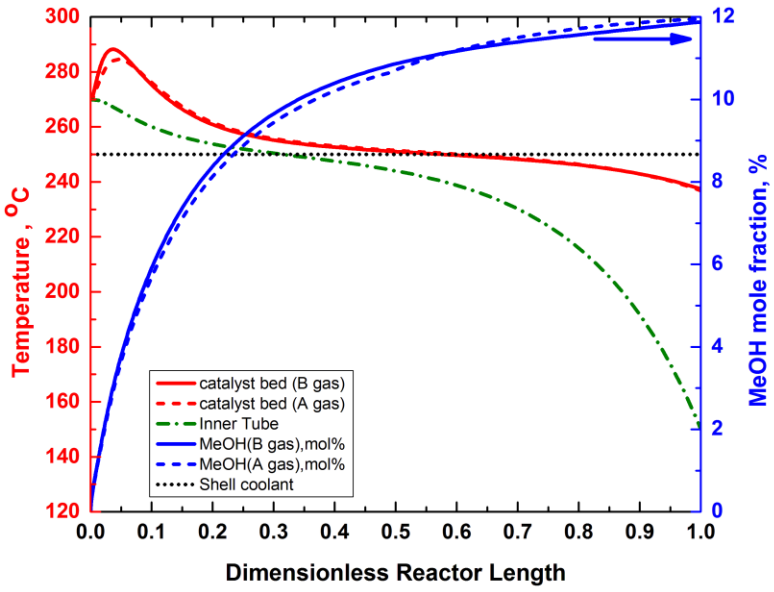

Figure 2.6: Effect of gas composition on gas temperature profile and methanol concentration (P=98 bar and SV=6000 h^{-1}).

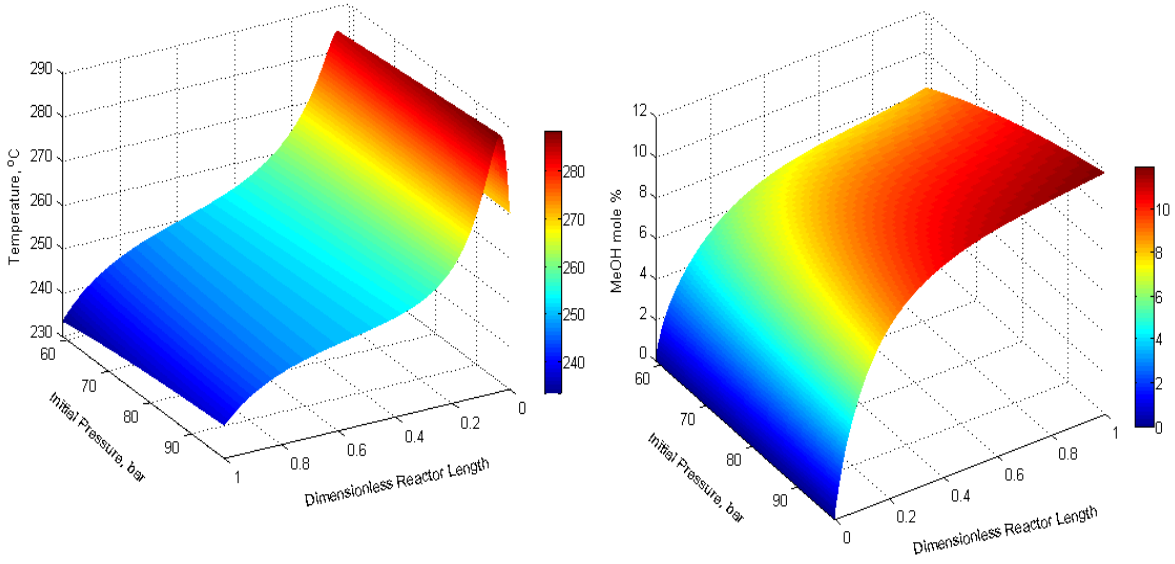

Figure 2.7: Effect of pressure on temperature profiles and methanol concentration along the reactor length.

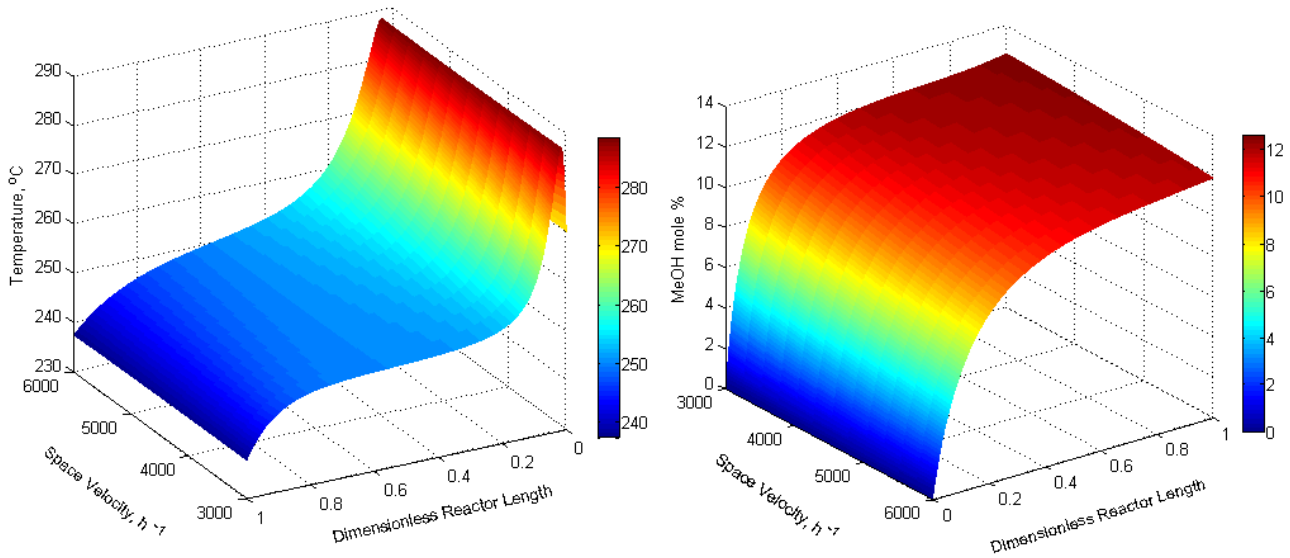

Figure 2.8: Effect of space velocity on temperature profiles and methanol concentration along the reactor length.

The simulations for different space velocities of feed gas are presented in Figure 2.8. Since the heat-transfer coefficients between particles and gas film within the catalyst tube depend upon space velocity, a lower space velocity leads to lower heat-transfer rate and then the temperature in the tube outlet becomes higher. As a result, the methanol concentration in the tube outlet also becomes higher. However, an extremely low space velocity results in thermal damage of the catalyst, especially at the inlet of the catalyst tubes and near the peak point.

CONCLUSION

The new reactor design has a capability to efficiently remove the heat generated by the exothermic reaction in methanol synthesis and its temperature profile is very favorable in terms of reaction rate and encourages the production of methanol. The methanol mole fraction profile increases gradually and reaches 11.92% and 11.36% for the double-tube exchanger and the conventional converter, respectively. Hence, the production of methanol is improved by 3%, compared to the conventional converter, while, at the same time, its operation is under mild conditions, especially at the end of the tube, allowing the catalyst to last longer. This leads to process intensification and allows for the use of a compact distillation step. In addition, this new design has the advantage of preheating the feed gas in the reaction, and the inner tubes will replace the feed gas preheater.

Chapter 3: Multi-objective optimization of methanol synthesis loop from synthesis gas via a multi-bed adiabatic reactor with additional inter-stage CO_2 quenching

ABSTRACT

The conversion of syngas derived from natural gas into methanol has been considered a relatively clean and environmentally friendly process. However, carbon dioxide is emitted as a result of using natural gas as fuel in the reformer furnace combustion zone to supply the heat required for endothermic reforming reactions. Carbon dioxide is a primary greenhouse gas emitted as flue gas from the reformer and has been contributing to global warming over the past few decades. Thereby, environmental regulations for new and existing industrial facilities have been enforced to mitigate the adverse effects of carbon dioxide emission. In this research, multiobjective optimization is applied for the operating conditions of the methanol synthesis loop via a multistage fixed bed adiabatic reactor system with an additional interstage CO_2 quenching stream to maximize methanol production while reducing CO_2 emissions. The model prediction for the methanol synthesis loop at steady state showed good agreement against data from an existing commercial plant. Then, the process flowsheet was developed and fully integrated with the Genetic Algorithms Toolbox that generated a set of optimal operating conditions with respect to upper and lower limits and several constraints. The results showed methanol production was improved by injecting shots of carbon dioxide recovered from the reformer at various reactor locations.

INTRODUCTION

The demand for alternative cleaner energy is growing rapidly, leading to an interest in methanol production and this demand is expected to increase further in the next decades. Methanol is extensively used as a raw material for formaldehyde production, methyl tert-butyl ether (MTBE) and acetic acid. It is also used in a direct methanol fuel cell (DMFC), where methanol is directly oxidized with air to water and carbon dioxide while producing electricity.[2,47] Methanol is expected to play a major role in our independence from the traditional gasoline derived from fossil fuel as an environmentally sustainable fuel. It has been reported by the U. S. Environmental Protection Agency (EPA) that switching gasoline to methanol would reduce 90% of the incidents caused by fuel.[48,49] Moreover, methanol can be used as a diesel replacement that does not produce particulates or soot when combusted. It also burns at a lower temperature than diesel; consequently, very low NO_x emission occurs.[1] The first synthetic methanol plant was introduced by Badische Anilin-und-Soda-Fabrik (BASF) in 1923;[12,13] the process synthesized methanol at 400 °C and 200 atm. During the 1960s, Imperial Chemical Industries (ICI) developed a low-pressure methanol process using a copper-based catalyst that completely altered the technology of methanol synthesis.[50] This process operates at 220-300 °C and 50-100 atm.

The ICI quench-cooled converter consists of a number of adiabatic catalyst beds installed in series in one pressure vessel.[10,51] A quench reactor is the most common methanol converter design and has been on line for more than 40 years and has proven its robustness and reliability for capacities ranging from 50 up to 3000 metric tons per day (MTPD).[52,53] In comparison with other pseudo isothermal converter types such as tubular (Lurgi), double-tube heat-exchange (Mitsubishi),[22,27,46] and radial isothermal (Methanol Casale), the quench converter produces more CO_2 emission and

requires a relatively larger catalyst volume as the temperature profile reaches the equilibrium maximum path.[51] Environmental regulations are aiming at reducing greenhouse gases especially carbon dioxide and nitrous oxide. The production of methanol for natural gas via steam methane reforming is a relatively clean process. However, a major source of CO_2 is generated in the reformer furnace combustion zoon as result of burning fuel gas to supply the heat required for the reforming reactions. As a consequence, CO_2 ends up being flue gas vented from the reformer to the atmosphere. Hence, a carbon dioxide recovery system is implemented to recover vented gas and utilize the CO_2 recovered as a feed to the upstream and/or downstream sides of the methanol synthesis to obtain the desired syngas molar ratio H_2/CO of 2.1 for producing methanol.

The modeling and optimization of methanol process have been addressed in the literature. For example, Lie et al.[54] presented a mixed integer programming (MIP) model of polygeneration technology (producing both electricity and methanol). Their case study considers China with the expectation that methanol would substitute 1-5% of the projected oil consumption from 2010 to 2035, and they concluded that polygeneration technologies are superior to conventional stand-alone technologies. Julian-Duran et al.[55] performed a techno-economic and environmental impact study of methanol produced from shale gas. Although a CO_2 recovery system was implemented and considered in their flowsheet analysis, CO_2 was either vented to the atmosphere or recycled back to the reforming section. In our analysis, the captured CO_2 is directly sent to methanol reactor to investigate methanol production enhancement. A multiobjective optimization framework is used to propose new operating conditions of low-pressure methanol synthesis loop via a multi-stage fixed bed adiabatic reactor system with additional inter-stage CO_2 quenching stream to maximize production while reducing CO_2 emissions.

PROCESS DESCRIPTION

A typical methanol process includes desulfurization of natural gas, steam reforming, methanol synthesis, and methanol refining.

Syngas Production

Production of syngas is traditionally performed through steam reforming of natural gas (methane) as follows:

$$CH_4 + H_2O \longrightarrow CO + 3H_2 \qquad (3.1)$$

Steam reforming of methane and water gas shift reactions (3.1) and (3.2) are taking place simultaneously. A high ratio of steam-to-carbon is required to suppress the coke formation (3.3) over the catalyst and to increase hydrogen production by the water gas shift reaction.[18]

$$CO + H_2O \rightleftharpoons CO_2 + H_2 \qquad (3.2)$$

$$2CO(g) \longrightarrow CO_2(g) + C(s) \qquad (3.3)$$

The SMR process consists of two major parts: a packed catalyst in tubes and a furnace to heat the reformer tubes. The desired syngas molar ratio for methanol synthesis is 2.1 according to the following formula, stoichiometric ratio (SR) = $(H_2\text{-}CO_2)/(CO+CO_2)$. As illustrated in Figure 3.1, the syngas produced in the reformer is passed through a heat exchanger, generating medium pressure steam, while the syngas is cooled down and then fed into a heat recovery system for further cooling to a mild temperature. The steam associated with syngas is condensed and used as boiler feed-water. Finally, dry syngas is compressed at 50-100 atm and then heated up to 200-250°C in order to prepare syngas for the methanol synthesis reactions.

Methanol Synthesis

A commercial methanol synthesis unit is generally licensed by various processes and catalyst suppliers. Each licenser has developed its own schematic diagram and catalyst structure. The heart of the ICI low pressure process is a quench converter packed with activated catalyst (Cu-ZnO/Al_2O_3) and operated under 10 MPa and 200–300°C. The ICI's low pressure methanol process with a quench reactor system is widely used, and therefore many methanol plants still use this technology.[50] This converter consists of multiple adiabatic beds in series where the synthesis reaction is quenched by additional cooled synthesis gas between the beds. Johnson Matthey Catalyst (formally ICI) collaborated with Methanol Casale to develop a new version of the converter that has the same quenching concept and is called Axial Radial converter (ARC). The ARC is a quench type converter, but with separate catalyst bed rather than a single continuous bed, in order to improve gas distribution. The methanol reactions in the low pressure synthesis loop can be summarized as:

$$CO + 2H_2 \rightleftharpoons CH_3OH \qquad (3.4)$$

$$CO_2 + 3H_2 \rightleftharpoons CH_3OH + H_2O \qquad (3.5)$$

$$CO_2 + H_2 \rightleftharpoons CO + H_2O \qquad (3.6)$$

Many methanol kinetic models proposed in the literature have been derived based on Langmuir-Hinshelwood mechanisms. However, Vanden Busshce and Froment experiments involved a commercial $Cu/ZnO/Al_2O_3$ catalyst under the typical industrial conditions.[56]

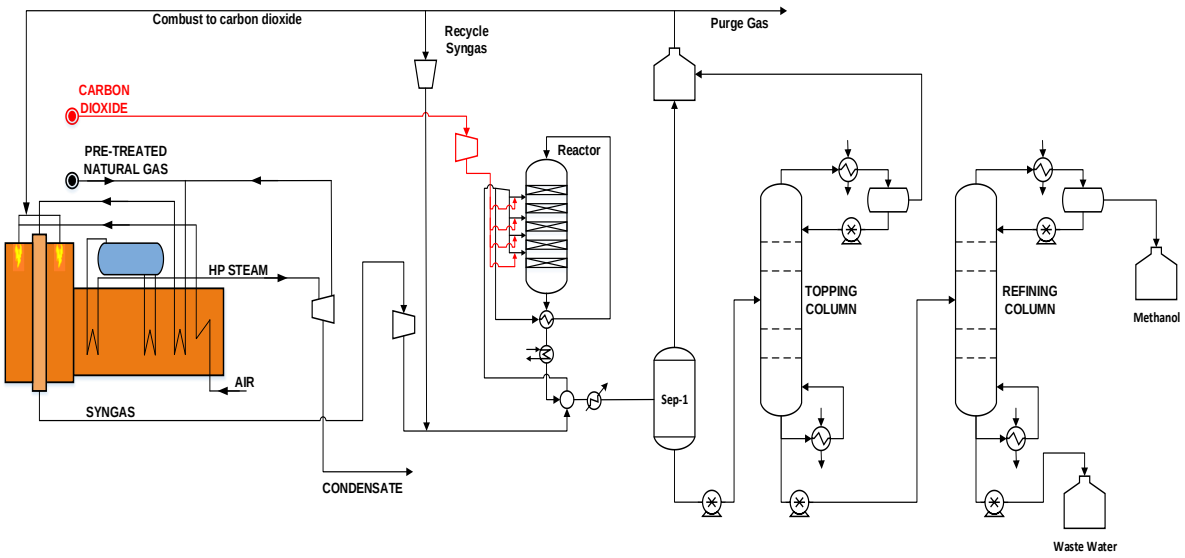

Figure 3.1: Process Flow Diagram of Methanol synthesis loop via Natural Gas Reforming.

The following expressions were obtained for the rate of methanol synthesis and the reverse water gas shift reaction:

$$r_{CH_3OH} = \frac{k_1 P_{CO_2} P_{H_2} \left[1 - \frac{1}{K_{eq1}} \frac{P_{H_2O}\, P_{CH_3OH}}{P_{H_2}^3\, P_{CO_2}}\right]}{(1 + K_{ad1} \frac{P_{H_2O}}{P_{H_2}} + K_{ad2}\, P_{H_2}^{0.5} + K_{ad3}\, P_{H_2O})^3} \tag{3.7}$$

$$r_{RWGS} = \frac{k_2\, P_{CO_2} \left[1 - K_{eq2} \frac{P_{H_2O}\, P_{CO}}{P_{H_2}\, P_{CO_2}}\right]}{\left[1 + K_{ad1}\, \frac{P_{H_2O}}{P_{H_2}} + K_{ad2}\, P_{H_2}^{0.5} + K_{ad3}\, P_{H_2O}\right]} \tag{3.8}$$

The equilibrium correlations are given as follows:

$$log_{10}(K_{eq1}) = \frac{3066}{T} - 10.592 \tag{3.9}$$

$$log_{10}(K_{eq2}) = -\frac{2073}{T} + 2.029 \tag{3.10}$$

The reaction rate and adsorption constants are of the Arrhenius form, with more details given elsewhere.[20-23] The reactants (CO, CO_2 and H_2) are supplied by makeup syngas. The converter consists of a pressure vessel with five catalyst beds, with inter-stage cooling shots accomplished by quenching as shown in Figure 3.2. Part of the fresh syngas enters the top bed, and the residue is entered as an inter-stage quench. This inter-stage quench gas is added to the gas reacting within the converter by means of gas mixing system. All the five beds are loaded with Haldor Topsøe methanol synthesis catalyst MK-101. By reduction of the catalyst, a theoretical amount of 125 kg H_2O is produced from one metric ton of catalyst. The catalyst activity will decrease slowly during normal operation although during a short period, approximately 1-3 months after initial start-up, the activity will decrease more rapidly than in the rest of the period. The catalyst has an expected life of four years provided that it is properly protected against poisons such as sulfur and chlorine.[59]

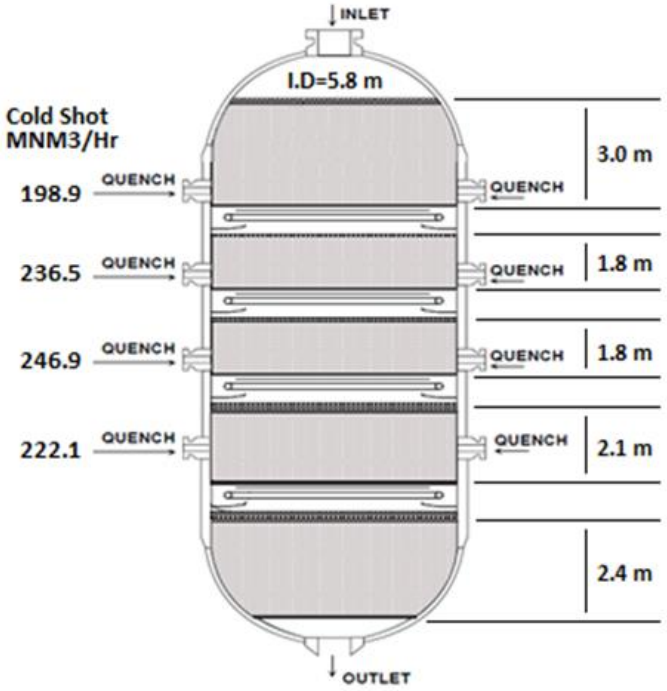

Figure 3.2: ICI Low pressure quench converter.

Subsequently, part of the syngas stream enters the reactor after preheating by the reactor effluent. The remaining syngas is used as quenched shot gas. The reactor effluent is cooled by heat exchange with the feed and boiler feedwater, and then syngas/crude methanol separation is carried out in a vessel under pressure. The gas is recycled after purging a small part of the feed to keep the level of impurities and hydrogen in the loop within limits. The purge gas is used as fuel for the reforming section. A mathematical model for adiabatic converter associated with inter-stage quenching is developed as follows. The mass and energy balances for the fluid phase are:

$$-\frac{1}{L}\frac{dF_i}{dx} + A_c\,\rho_b \sum_{n=1}^{N_{rxn}} v_{n,i}\,\eta_n r_n = 0 \tag{3.11}$$

$$u_g \rho_g C_{pg}\frac{dT}{dx} + \rho_b \sum_{n=1}^{N_{rxn}} \left(-\Delta H_{r,n}\right)\eta_n r_n = 0 \tag{3.12}$$

where F_i is the flow rate of component i and T is the temperature of the reactants inside the converter. The Ergun equation is used to calculate pressure drop through the catalyst packed beds.

$$\frac{1}{L}\frac{dP}{dx} = -\frac{G}{\rho_g\, g_c\, d_p}\left(\frac{1-\phi}{\phi^3}\right)\left(\frac{150(1-\phi)\mu_g}{d_p} + 1.75G\right) \tag{3.13}$$

The initial conditions are: $x = 0,\ F^i(0) = F^i_{inlet}, T(0) = T_{inlet}\ and\ P(0) = P_{inlet}$.

The methanol conversion reactions are exothermic; thereby the heat of reaction is removed in each stage to increase the conversion per pass through the reactor.

The Methanol Refining

The crude methanol from methanol synthesis is purified by the use of distillation columns. According to U. S. Federal grades of methanol, there are two methanol grades: grade AA and grade A. The methanol minimum weight of grade AA and grade A are the same 99.85%, whereas water maximum weights are 0.1% and 0.15% respectively. Typically grade A of crude methanol requires two distillation columns, whereas grade AA requires three distillation columns. The reactor effluent is cooled by heat exchange with the fresh syngas stream and boiler feedwater, and then unreacted syngas/crude methanol separation is carried out in a vessel under pressure. The unconverted syngas is recycled to the converter through a circulator compressor. A small purge of unreacted syngas is taken from the recycled gas to maintain a minimum level of impurities and hydrogen in the loop and used as fuel in the reformer. The condensed product (water/methanol) then proceeds to the crude methanol storage tank after being flashed at a pressure above atmospheric pressure to remove gases physically dissolved at the separation pressure. The crude methanol is sent to a distillation column system normally consisting of two columns: the first column operates at elevated pressure and removes syngas and hydrocarbon impurities from the methanol/water mixture; the second column separates methanol from water at atmospheric pressure. The crude methanol is pumped from the storage tank into a topping column for removal of light impurities, such as methyl formate, in the overhead. This column is operated under elevated pressure, slightly higher than atmospheric pressure.[21] The bottom stream from the topping column is fed into the refining column where the purified methanol is separated as a top stage distilled product and the wastewater is discharged from the system.

METHODOLOGY AND SOLUTION STRATEGY

An end-user interface is developed to employ a simulation-based multiobjective optimization scheme (a combination of Microsoft Excel (MS) Visual Basic for Applications (VBA) macro and optimization technique developed in Matlab). Then, it is used to optimize the methanol process by means of Aspen Plus flowsheet simulation software. To accomplish this task, a rigorous reactor model is developed in Aspen Custom Modeler and imported into Aspen Plus. The Soave-Redlich-Kwong (SRK) equation-of-state is implemented to improve phase equilibrium calculations in water-hydrocarbon systems and equation-based calculations by using composition independent fugacity.[59] Most of the units involved in the process are successfully described by the available built-in models in the Aspen Plus model library. A nonrandom two-liquid (NRTL) thermodynamic package is used for predicting the VLE of the mixture of light hydrocarbon and Methanol/water with high accuracy. The Aspen Plus user interface is an ActiveX Automation Server, formerly known as object Linking and embedding (OLE) automation, which enables a VBA macro to interact with the process flowsheet by sending inputs and receiving results. This feature of integrating Aspen Plus with Microsoft application allows the Matlab optimization toolbox to manipulate operational variables and receive the response from Aspen Plus through an Excel spreadsheet. Errors may happen in calling or accessing Aspen Plus object. Thus, it is important to write error handling statements for the code to resume the process of communicating thru an automation interface.[61] The structure of the end-user interface and the links between MS Excel, Aspen Plus, and Matlab are illustrated in Figure 3.3. In the first run, the input data can be provided manually including the bound of each variable and the constraints.

Then the data passes to MS Excel to be implemented in the Aspen Plus flowsheet. The outcome of this run provides new input data for the next step.

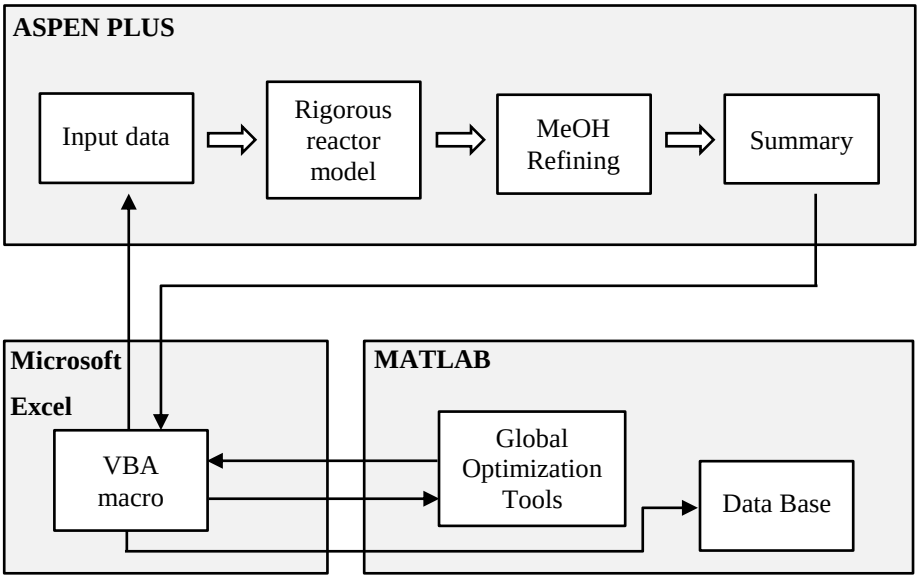

Figure 3.3: sketch of the programs integration and data exchange.

The model is kept running until the solver's stopping criteria are achieved. The results are displayed in the Matlab command window and saved in Matlab files for further analysis. The complete process of methanol synthesis involving catalytic reaction, separation and purification has been simulated in Aspen Plus as shown in Figure 3.4. Whilst all these steps are important, the conversion of syngas to methanol is the most critical step since all the existing equipment are being used to their fullest advantage by examining operating data to identify equipment bottlenecks. Observing the importance of the reactor unit, this study investigates the benefits of adding an extra CO_2 stream to quench more CO_2 gas along the reactor length. The optimization objective, variables and constraints are defined as follows:

$$Maximize\ f_1 = F_{S20,MeOH} \tag{3.14}$$

$$Maximize\ f_2 = \left(F_{S1,CO2} + F_{S31,CO2} + F_{S25,CO2}\right) - F_{S14,CO2} \quad (3.15)$$

where streams (S20, S1, S31, S25 and S14) are shown in Figure 3.4. The functions for optimization are methanol production rate and CO_2 emission reduction. The reduction of CO_2 emission is defined as the net of CO_2 consumed inside the reactor, considering the extra amount of CO_2 quenched into the reactor stages. For optimization of methanol synthesis via a multi-bed adiabatic reactor, the decisions were made based on the operating variables of an existing plant and the possibility of adding an extra quenching stream to inject more CO_2 along the reactor. The methanol plant under investigation has a production capacity of 2682 MTPD.[62] These variables with their corresponding bounds are:

$0<F_{S25,CO2}<5000$, kmol/hr (3.16)

$50<T_{S25}< 200$, ^{o}C (3.17)

$0\leq X_1\leq 1$, split fraction to stream S26 (3.18)

$0\leq X_2\leq 1$, split fraction to stream S27 (3.19)

$0\leq X_3\leq 1$, split fraction to stream S28 (3.20)

$$\sum_{i=1}^{4} X_i = 1 \quad (3.21)$$

These decision variables are subjected to one path constraint stating that the temperature of the catalyst beds must be less than 543K to avoid severe catalyst deactivation and decreased selectivity.

$$T_{max} < 543\ K \quad (3.22)$$

The optimization results were performed on a computer with 2.5 GHz dual-core Intel Core i5 and 16 GB memory to facilitate accessing and storing large amounts of data and to prevent “out of

memory" error messages appearing due to the a large number of runs of multi-objective genetic algorithm solver '*gamultiobj'* in the Matlab optimization toolbox,[63] which uses a controlled elitist genetic algorithm (a variant of NSGA-II).[64,65] Some important options must be set suitably in the genetic algorithm (GA) solver. These include the number of variables, fitness functions, constraints and two elitism options '*ParetoFraction'* and '*DistanceFcn'* which are used to limit the number of individuals on the Pareto front (elite members) and to maintain diversity by controlling the elite members of the population as the algorithm progresses, respectively.

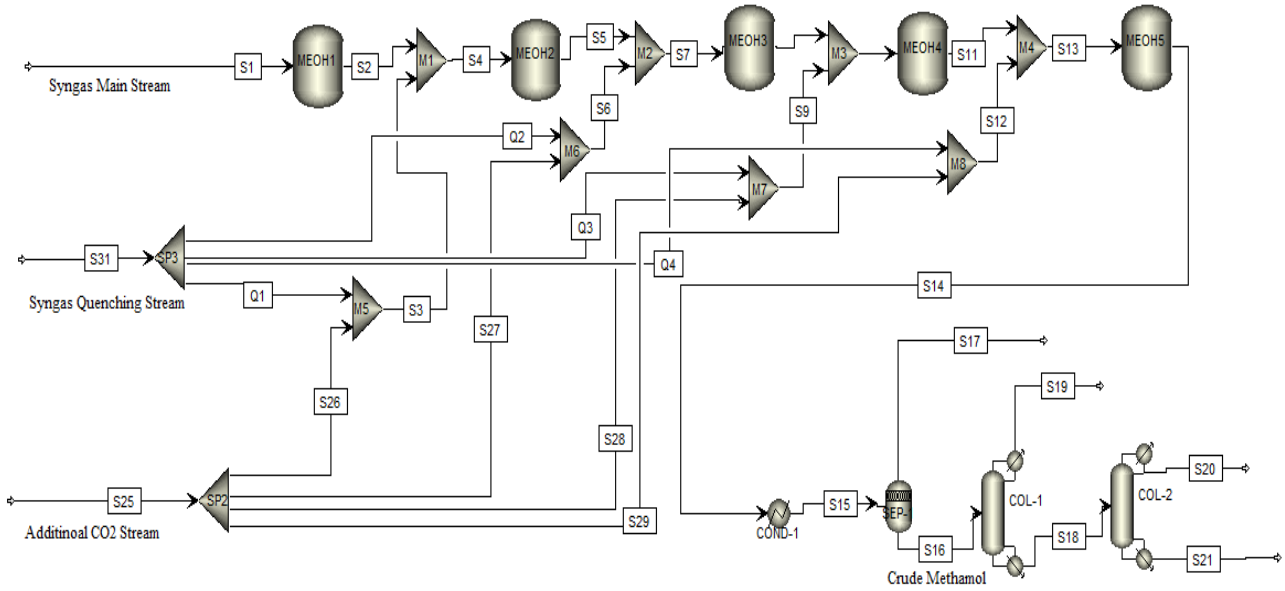

Figure 3.4: Aspen Plus flowsheet of methanol synthesis loop with additional inter-stage CO_2 quenching.

Table 3.1 shows the parameters that were tuned experientially to improve the smoothness and diversity of the Pareto optimal solutions. Other options were defined as the default.

Table 3.1: Parameters of gamultiobj function –multiobjective optimization using Genetic Algorithm.

parameters	**Value**
Population type	Double vector
Population size	200
Crossover fraction	0.8 -default
Elite count	
Fitness functions	Intermediate, ratio=1
Mutation fraction	Use constraint dependent default
generation	Use default: 200*number of
ParetoFraction	Use default :0.35
DistanceFcn	The crowding distance

RESULTS AND DISCUSSION

A generic ICI's methanol synthesis process flow diagram has been developed, including an adiabatic quench type reactor with five catalytic beds separated by four inter-stage cold shot distributes. These distributors are designed to give a good mixing between injected cold shots and the hot gas flows through the reactor. The simulation model was validated against real industrial plant data that provides only the temperature between beds and the compositions at the end of the reactor. Figure 3.5 (a) and (b) show that both temperature and methanol conversion results are in good agreement with real plant data.

The methanol concentration is reduced while the fresh synthesis gas is injected through the distributors and consequently more catalyst being required to achieve a high methanol yield per bed. In order to demonstrate this characteristic, methanol concentration along the reactor length and the equilibrium concentration of methanol were plotted versus the corresponding reaction temperature in Figure 3.6. The path of methanol concentration revolves around the equilibrium-temperature trajectory to ensure the maximum methanol yield is achieved in each stages of the reactor.

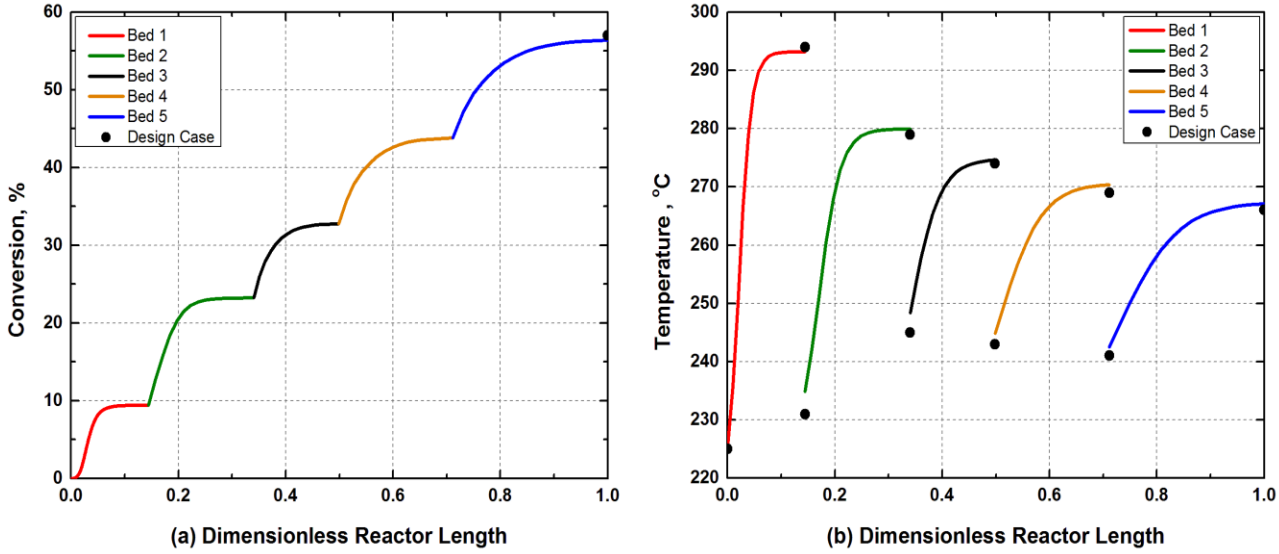

Figure 3.5: Temperature and conversion profiles versus dimensionless reactor length.

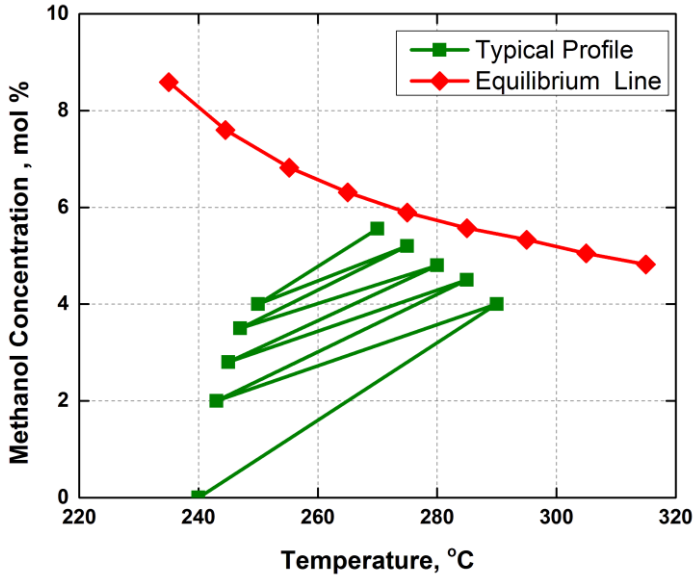

Figure 3.6: Mole percent methanol versus temperature diagram in Quench Converter.

The optimization of methanol synthesis has been carried out with the elitist non-dominated sorting genetic algorithm (NSGA-II). The design and operating conditions of the synthesis loop are taken from published industrial data and used to validate the results of the model to ensure

reliability and robustness. The additional CO_2 injected to the system and the splitting ratios are used as decision variables, whereas the reactor design, including the injection location, and design of other units are fixed. Figure 3.7 clearly shows that there is no solution that is the best with respect to methanol production and carbon dioxide consumption. Instead a set of solutions which are superior to the best of solutions in the search space, these solutions are known as Pareto-optimal solutions or non-dominated solutions.

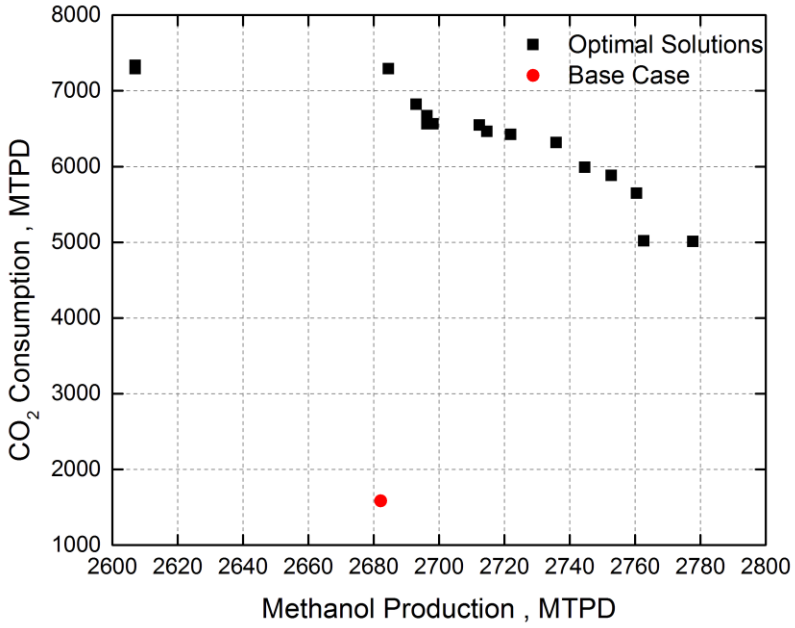

Figure 3.7: Pareto optimal set obtained from dual maximization of methanol production and CO_2 consumption.

The pareto optimal results reveal clearly the trade-off between the carbon dioxide consumed and the methanol produced. If the operator desires to operate the reactor with conditions that minimize CO_2 emission (in other words, consuming more CO_2 inside the synthesis loop) then more waste water will be produced and almost no extra methanol can be produced.

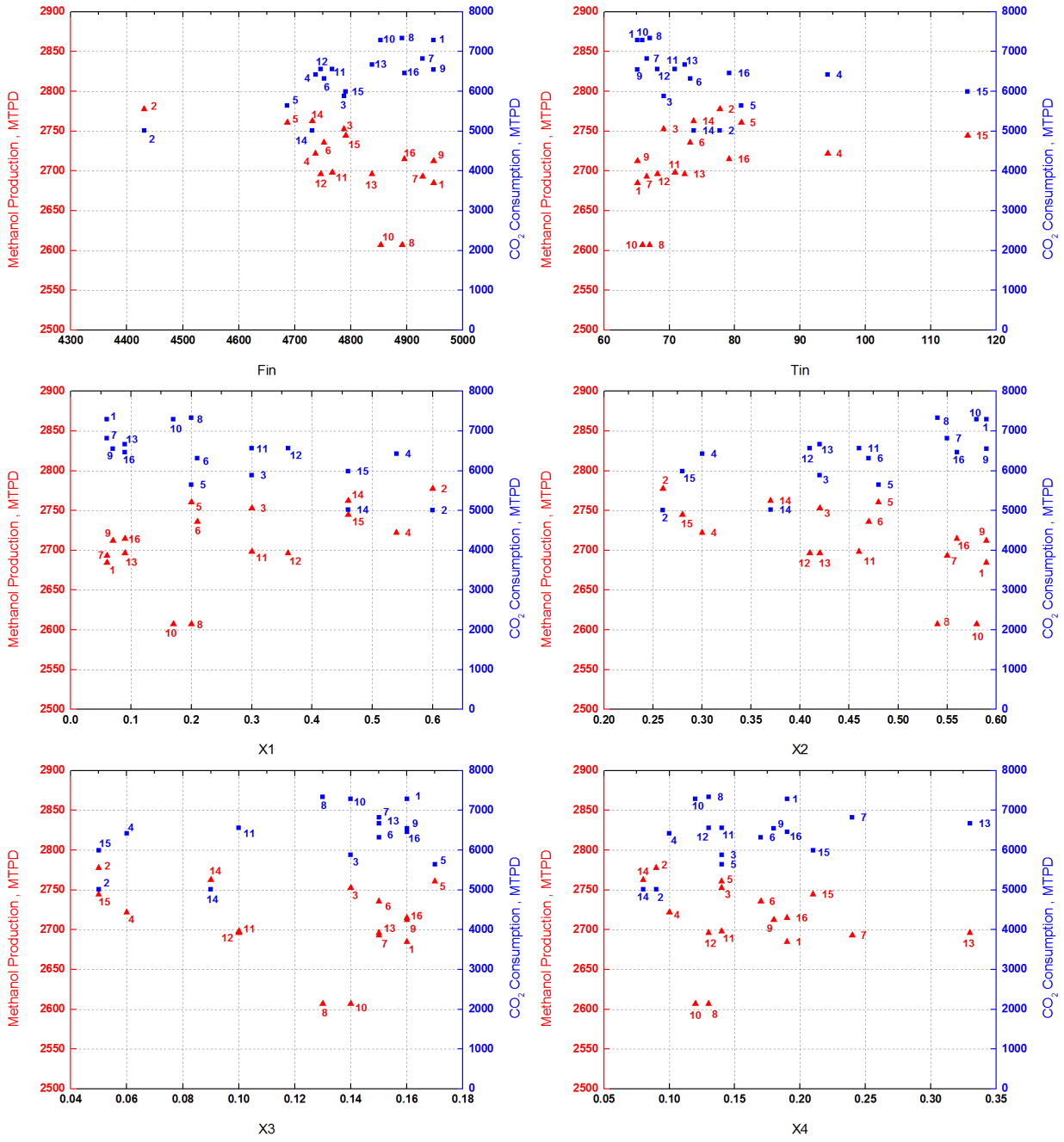

Figure 3.8: (a)–(f) Decision variables corresponding to pareto optimal set in Fig. 3.7, X_1, X_2, X_3 and X_4 are the split fractions of stream S25 to S26, S27, S28 and S29, respectively.

However, the highest methanol generated by the quench converter is ~2778 MTPD when ~5010 MTPD of carbon dioxide is consumed. This leads to an improvement of the plant production by

3% as well as preventing 3430 MTPD of CO_2 from being released to the atmosphere. Figure 3.8 (a, b, c, d and f) shows the values of the decision variables corresponding to the Pareto domain of Figure 3.7 plotted versus the objectives. These decision variables have a great influence on several factors that control reactor performance; more CO_2 consumed in the production of methanol reactions increased the temperature and produced CO, which in turn was consumed in the production of methanol.

CONCLUSION

The multi-objective optimization problem of ICI's low pressure methanol process operating conditions has been performed for efficient methanol production with reduced CO_2 emission. To tackle this problem, the elitist non-dominated sorting genetic algorithm (NSGA-II) is adopted to determine the optimum amount of captured CO_2 that can be utilized, the favorable temperature and the splitting factor of each quenching stream. The potential possibilities of improving the process were analyzed using a rigorous model integrated with a generic process flowsheet to obtain necessary comparative results. In contrast to the base case of industrial plant, the results have illustrated different operating conditions to operate the plant at different carbon dioxide consumption levels and production rates. It is shown that the highest Methanol generated by the quench converter is ~2778 MTPD when ~5010 MTPD of carbon dioxide is consumed. This leads to an improvement of the plant production by 3% as well as preventing 3430 MTPD of CO_2 from being released to the atmosphere. The main advantage of applying multiobjective optimization is the ability to choose one of the optimal solutions based on a good knowledge of the process and the preferred condition.

Chapter 4: Dynamic Optimization of Lurgi Type Methanol Reactor Using Hybrid GA-GPS Algorithm: The Optimal Shell Temperature Trajectory and Carbon Dioxide Utilization

ABSTRACT

At present, methanol is mostly produced from syngas, derived from natural gas through steam methane reforming (SMR). In a typical methanol production plant, unreacted syngas is recycled for mixing with natural gas and both used as fuel in the reformer furnace resulting in carbon dioxide (CO_2) emissions from the flue gases emitted into the atmosphere. However, CO_2 can be captured and utilized as feedstock within the methanol synthesis process to enhance the productivity and efficiency. To do so, dynamic optimization approaches to derive the ideal operating conditions for a Lurgi type methanol reactor in the presence of catalyst deactivation are proposed to determine the optimal use of recycle ratio of CO_2 and shell coolant temperature without violating any process constraints. In this context, this study proposes a new approach based on a hybrid algorithm combining genetic algorithm (GA) and generalized pattern search (GPS) derivative-free methodologies to provide a sufficiently good solution to this dynamic optimization problem. The hybrid GA-GPS algorithm has the advantage of sequentially combining GA and GPS logics; while GA, as the most popular evolutionary algorithm, effectively explores the landscape of the fitness function and identify promising basins of the search space, GPS efficiently search existing basins in order to find an approximately optimal solution. The simulation results showed that implementing the shell temperature trajectory derived by the proposed approach with 5% recycle ratio of CO_2 enhanced the production of methanol by approximately 2.5 % compared to the existing operating conditions.

INTRODUCTION

Carbon dioxide is the primary greenhouse gas emitted to the atmosphere through fossil fuels (coal, natural gas, oil) consumption for energy supply and transportation. In addition, many industrial processes produce CO_2 emission either as a result of fossil fuel combustion to create heat and steam and/or as a byproduct of chemical reactions.[66] For instance, steam methane reforming (SMR) is widely used to produce syngas from natural gas, where reforming reaction takes place inside catalyst filled tubes and heated externally by firing fuel in a burner located in the furnace chamber.[67] Flue gases are discharged through an exhaust at the top of furnace to a heat recovery system where feed fuel and combustion air are preheated, and steam is generated. In the process of burning natural gas using air as an oxidant, the flue gas usually consists of mostly nitrogen followed by carbon dioxide with nearly 10−25 volume percent of the flue gas. It also contains small percentage of some pollutants, such as soot, carbon monoxide, nitrogen oxide.[68] Consequently, research studies on carbon dioxide utilization focus on developing novel approaches for mitigating the contributions of CO_2 emissions to global warming and ocean acidification by developing beneficial uses of CO_2 in such areas where geologic storage of CO_2 may not be the best option.[69] The advantage of CO_2 fixation over CO_2 disposal is that the production of chemicals with high economic value is possible.[70]

The reaction of carbon dioxide and methane in absence of steam (4.1), known as dry reforming of methane (DRM), to form syngas is the most appealing approach to convert two inexpensive materials into useful chemical building blocks.[71]

$$CH_4 + CO_2 \rightarrow 2CO + 2H_2 \qquad \Delta H_{298\,K} = 247.3\ \text{kJ mol}^{-1} \qquad (4.1)$$

A challenging problem in commercialization of dry reforming process is that the reaction condition is more favorable for other side reactions such as methane decomposition (4.2), boudouard equilibrium (4.3).[72]

$$CH_4 \rightarrow C + 2H_2 \qquad \Delta H_{298\,K} = 74.8\ \text{kJ mol}^{-1} \qquad (4.2)$$

$$2CO \rightarrow C + CO_2 \qquad \Delta H_{298\,K} = -172.5\ \text{kJ mol}^{-1} \qquad (4.3)$$

Coke deposition occurs by the exothermic boudouard reaction and the endothermic cracking of methane which leads to severe catalyst deactivation and the need for premature catalyst change-out.[73,74] CALCOR process uses a special catalyst for reacting dry CO_2 with natural gas, liquid petroleum gas (LPG), and syngas to produce high purity carbon monoxide that contains less than 0.1% methane and H_2/CO ratio as low as 0.4.[75,76] combination of steam methane reforming and dry methane reforming (SMR+DRM) of natural gas is a competitive process to the conventional SMR process. SMR+DRM produces the best syngas ratio for production of liquid fuels with 2-2.1 H_2/CO molar ratio; whereas, SMR of natural gas produces syngas with a H_2/CO molar ratio of slightly above 3.[20] Regardless of its advantages, SMR+DRM process has not been matured yet and still suffer from coking, severely shortening the lifetime of the applied catalysts. As the DRM technology has not been widely implemented for reducing CO_2 emission, alternative approaches to address this issue are still under ongoing investigation.[77] Chemical recycling of CO_2 to renewable fuel, such as methanol, offers a future transportation fuel.

G. Olah and his research group developed an improved Cu/ZnO based catalyst for methanol synthesis from CO_2 and H_2 at similar operating conditions and deactivation rate to those of commercial catalysts for syngas-based methanol synthesis.[1,2] The first CO_2-to-methanol recycling plant, (George Olah Renewable Methanol Plant) is operated in Iceland by Carbon Recycling

International (CRI).[3] This plant uses available local geothermal energy (hot water and steam) to supply the electricity needed to produce pure H_2 by water electrolysis process with a daily capacity of 10 ton/day. The present technologies of water electrolysis have an efficiency of 50%-80% and require 50-79 KWh/kg of H_2; hence they cost 3 to 10 times more than steam methane reforming even with a traditional method of generating electricity.[78]

The direct conversion of natural gas is more feasible and cost-effective at an industrial level than burning the fuel to generate electricity needed to electrolyze water and then producing hydrogen.[79] For an SMR-based methanol plant, H_2/CO molar ratio is obtained close to 3 which are not optimal for methanol synthesis process. Therefore recycling CO_2 back to the reformer feed gas can be an option to increase methanol production by adjusting the stoichiometry of the make-up gas, which increases the reformer heat duty while reducing the amount of waste water discharged from the distillation system. A case study presented by Reddy el al.(2014) showed that the methanol plant capacity can be expanded approximately 20% by recovering sufficient CO_2 from steam reformer stack and recycle it as feedstock to the SMR.[80] However, recycling CO_2 to the reformer feed-gas increases the demand of supplying more heat.

An alternative option is recycling CO_2 into the syngas compressor suction feed rather than reformer feed. In previous research, we have concluded that around 3% improvement in the plant production capacity can be achieved by injecting additional inter-stage CO_2 into ICI's multi-bed adiabatic reactor.[5] The objective of this study is using dynamic optimization to derive the optimal recycle ratio of CO_2 and shell temperature trajectory of an industrial methanol lurgi-type reactor during four years catalyst lifetime. We kept the recycle ratio of CO_2 within the design limit of the plant (maximum 10%) and the peak bed-temperature less than or equal to 543K and, then

analyzed the effects of these decision variables on the reactor performance and the catalyst activity.

MODEL DEVELOPMENT

Consider a mid-size methanol plant, e.g., up to 2500 ton/day, employs a steam methane reformer with an external source of hot gas to heat tubes in which catalytic reforming reactions take place. The feedstock to the reformer is a mixture of steam and natural gas with a typical steam-to-carbon ratio of 3:1 to avoid carbon deposition on the catalyst surface.[81] Steam and methane are converted to syngas at a high temperature and an elevated pressure.. The syngas is then mixed with recycled unreacted gas, pressurized in a compressor until the operational pressure of methanol synthesis process is achieved, and then fed to a water-cooled tubular reactor. The tubes packed with catalyst are externally cooled by boiler-water and a nearly isothermal temperature profile is formed in the catalyst bed. This type of reactors aims at recovering the heat of methanol synthesis reactions in the form of high pressure steam to the maximum possible extent. Figure 4.1 shows the schematic diagram of the methanol synthesis process. Methanol synthesis from syngas over $Cu/ZnO/Al_2O_3$ catalyst composed of three main equilibrium reactions:

$$CO + 2H_2 \rightleftharpoons CH_3OH \qquad \Delta H_{298\,K} = -91\ \text{kJ mol}^{-1} \tag{4.4}$$

$$CO_2 + 3H_2 \rightleftharpoons CH_3OH + H_2O \qquad \Delta H_{298\,K} = -50\ \text{kJ mol}^{-1} \tag{4.5}$$

$$CO_2 + H_2 \rightleftharpoons CO + H_2O \qquad \Delta H_{298\,K} = +41\ \text{kJ mol}^{-1} \tag{4.6}$$

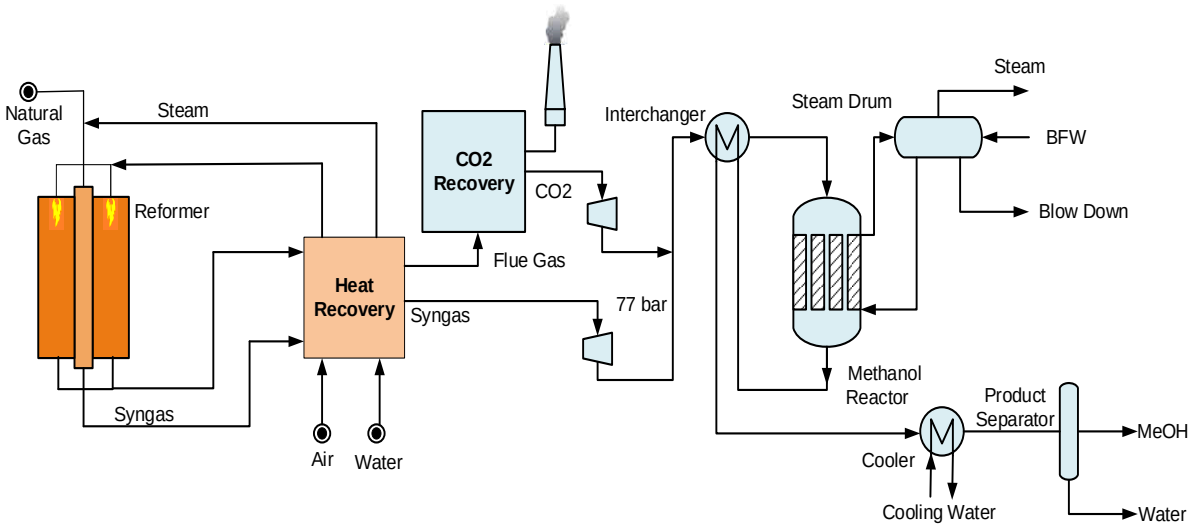

Figure 4.1: Scheme of the methanol synthesis loop.

Reactor model

The methanol synthesis reactor studied here is of Lurgi-type used in Shiraz Petrochemical Company.[82] A one-dimensional heterogeneous reactor model is used to simulate the performance of industrial Lurgi-type methanol reactor. It employed a two phase model in which heat transfer through the solid- and fluid phases is considered separately.[83] The continuity and energy equations for solid and fluid phases are expressed as follows:[36]

Continuity equations:

$$\varepsilon_b \frac{\partial C_i}{\partial t} = -u_z \frac{\partial C_i}{\partial z} + k_{g,i} a_v (C_i^s - C_i) \qquad \forall\, z \in (0, L], t \in (0, t_f]\,, i = 1,2, \dots, N_c \tag{4.7}$$

$$\varepsilon_s \frac{\partial C_i^s}{\partial t} = R_i(C_i^s, T^s) - k_{g,i} a_v (C_i^s - C_i)\ \forall\, z \in (0, L], t \in (0, t_f]\,, i = 1,2, \dots, N_c \tag{4.8}$$

Energy equations:

$$\rho_f c_{p,f} \frac{\partial T}{\partial t} = - u_z \rho_f c_{p,f} \frac{\partial T}{\partial z} + h_f \, a_v (T^s - T) + 4 \frac{U_w}{D_i} (T_{shell} - T) \;\; \forall \, z \in (0, L], t \in (0, t_f] \tag{4.9}$$

$$\rho_s c_{p,s} \frac{\partial T^s}{\partial t} = R_T (C_i^s, T^s) - h_f a_v (T^s - T) \;\; \forall \, z \in (0, L], t \in (0, t_f] \tag{4.10}$$

The reactions rates and heat of reactions terms are:

$$R_i (C_i^s, T^s) = \rho_b \tilde{a} \sum_{j=1}^{N_{rxn}} v_{ij} r_j (C_i^s, T^s) \;\; , i = 1,2, \dots, N_c \tag{4.11}$$

$$R_T (C_i^s, T^s) = \rho_b \tilde{a} \sum_{j=1}^{N_{rxn}} r_j (C_i^s, T^s) \left(- \Delta H_{r,j} (T^s) \right) \;\; , i = 1,2, \dots, N_c \tag{4.12}$$

Boundary and initial conditions:

$$C_i = C_{i,in} \; ; T = T_{in} \quad @ \; z = 0, t \in [0, t_f] \tag{4.13}$$

$$C_i = C_{i,0} \; ; \; T = T_0 \quad @ \; t = 0, z \in (0,1] \tag{4.14}$$

$$C_i^s = C_{i,0}^s ; \; T^s = T_0^s \quad @ \; t = 0, z \in [0,1] \tag{4.15}$$

The methanol production rate can be formulated as:

$$Production = N_{tubes} \, A_c \, u_z \, Mw_{MeOH} \, C_{MeOH}|_{z=L} \tag{4.16}$$

In this set of equations C_i stands for concentration of reactant i. The feed specifications and catalyst characteristics of methanol synthesis reactor are presented in Table 4.1.

Reaction kinetics

Three overall reactions (4.4)-(4.6) (hydrogenation of CO and CO_2, and the reverse water-gas shift) are possible occurred in methanol synthesis. Several studies proposed kinetic models of methanol synthesis.

Table 4.1: Feed composition and catalyst specifications of industrial plant methanol synthesis reactor.

Parameters	**Value**
Feed Composition	
Inlet flow rate, (mol s^{-1})	0.64
Mole Fraction,%	
CH_3OH	0.50
CO	4.60
CO_2	9.40
H_2	65.90
H_2O	0.04
CH_4	10.26
N_2	9.30
Design and Catalyst Specifications	
Inlet pressure, bar	76.98
Length of the reactor, m	7.022
ε_b	0.39
ρ_B, kg m^{-3}	1132
a_v, m^{-1}	626.98
Tube inner diameter, mm	38
Number of Tubes	2962

In this study, we used Langmuir–Hinshelwood–Hougen–Watson (LHHW) type reaction kinetic model of Brussche and Froment because it is the only model based on experiments involving a commercial ICI 51-2 $Cu/ZnO/Al_2O_3$ catalyst that is grounded and diluted for the sake of preventing the diffusion resistance and accurately controlling the pseudo-isothermicity of the reaction.[19] The corresponding rate expressions for hydrogenation of CO and CO_2, and reversed water–gas shift reactions are:

$$r_{CH_3OH} = \frac{k_1 P_{CO_2} P_{H_2} \left[1 - \frac{1}{K_{eq1}} \frac{P_{H_2O}\, P_{CH_3OH}}{P_{H_2}^3\, P_{CO_2}}\right]}{(1 + K_{ad1} \frac{P_{H_2O}}{P_{H_2}} + K_{ad2}\, P_{H_2}^{0.5} + K_{ad3}\, P_{H_2O})^3} \quad (4.17)$$

$$r_{RWGS} = \frac{k_2\, P_{CO_2} \left[1 - K_{eq2} \frac{P_{H_2O}\, P_{CO}}{P_{H_2}\, P_{CO_2}}\right]}{\left[1 + K_{ad1}\, \frac{P_{H_2O}}{P_{H_2}} + K_{ad2}\, P_{H_2}^{0.5} + K_{ad3}\, P_{H_2O}\right]} \quad (4.18)$$

Where P_i is the partial pressure of component i in bar and the reaction rates are cacluated per kilogram of catalyst (kmol/kg.cat s). The parameters of the equations including the reaction rate constants, adsorption equilibrium constants, and reaction equilibrium constants are given elsewhere.[56]

Deactivation model

The sulfur components normally present in the natural gas feedstock must be removed to prevent poisons and subsequent quick deactivation of the reforming process and methanol synthesis catalysts. Under normal operation conditions, deactivation of $Cu/Zn/Al_2O_3$ catalyst is slow and only caused by thermal sintering, which occurs by the migration of copper crystals to larger agglomerates.[84] In preparing a fresh catalyst, it is first activated by reduction conventionally carried out with hydrogen. Once reduction reaction is complete, the fresh catalyst is used immediately in methanol synthesis by replacing the hydrogen stream by syngas stream and implementing changes in pressure, temperature and space velocity, as desired. The fresh catalyst activity declines in the first 20 hours by as much as 60%.[85] The adjusted deactivation model developed by Hanken was found to give results in good agreement with industrial operating conditions.[86] The rate of change in the activity of $Cu/Zn/Al_2O_3$ catalyst based on this model is given as follows:

$$\frac{da}{dt} = -K_d \, exp\left(\frac{-E_d}{R}\left(\frac{1}{T} - \frac{1}{T_R}\right)\right) a^5 \quad \forall \, t \in (0, t_f] \tag{4.19}$$

$$\tilde{a} = 1 - \frac{a_0 - a}{a_0} \tag{4.20}$$

Where T_R =513 K, E_d = 91270 J mol^{-1}, and K_d = 0.00439 h^{-1} are the reference temperature, activation energy, and deactivation constant of the catalyst, respectively. An initial value a(t=0) of 0.4 was assumed. A relative activity started at one is used to find the reaction rate.

Simulation

A mathematical treatment of the governing model equations, eq. (4.7)-(4.20), is carefully addressed before solving them. Since the catalyst activity is rapidly declined within the first 20 hours of start-up operation, the transient behavior of the reactor system is not of interest to our investigation and the numerical solutions are performed in two consecutive stages; steady state stage followed by dynamic stage.

Steady State

The above heterogeneous model, eq. (4.7)-(4.18), consists of a set of partial differential equations. In steady state models, theses equations are reduced to ordinary differential equations (ODEs) and algebraic equations by eliminating the left hand sides of the equations (unsteady state terms) and assuming the catalyst activity is unity. This system of equations is initially solved by decoupling the fluid and solid phase in such a way that the solution of system is obtained in two consecutive stages, where the solid phase nonlinear algebraic equations is solved by using the powerful Newton-Raphson method and subsequently the obtained values of solid phase variables are used in the fluid phase ODEs. ODEs equations are often solved by Runge-Kutta fourth-order (RK4) or

Gear's methods. Both methods incorporate an error control scheme to automatically adjust the step-size, providing good accuracy generally. Gear's method is of more sophisticated scheme ensuring reliable convergence and accuracy, and thus it is an effective solver for solving a stiff ODEs system.[87] Fortunately, the ODEs system considered herein is not stiff system and therefore RK4 scheme is applied to provide an accurate solution with reduced computational costs. The purpose of solving the system by this technique is to: 1.determine the initial conditions for temperature and concentrations to be used for dynamic simulation described in the next section. 2. It is crucial to assure that the integration step size used in the finite difference method guaranties an acceptable accuracy of the solution and good enough to be adopted later to solve the dynamic simulation. Considerable attention has been directed towards the discretization of the convection terms and incorporation of source terms, transfer terms, and the boundary conditions into the numerical solution scheme. The scheme is an explicit approximation of the ODEs system, which usually cuts down the computational time. However, the implementation of the explicit method leads to restrictions on the step size because of numerical stability concerns. For discretization of the ODEs system, we imposed the scheme to obey the following stability condition:[88]

$$\frac{d\vec{u}}{dz} = f(z,\vec{u}) \text{ with } \vec{u}(0) = u_0 \qquad (4.21)$$

where $d\vec{u}/dz$ are the derivatives of concentrations and temperature with respect to space-direction in fluid phase equations (4.7) and (4.9), the Jacobian matrix of the set of functions f is defined as:

$$J_f = \left[\frac{\partial f_i}{\partial u_j}\right], i = 1,2,\dots,N_{eqs}, j = 1,2,\dots,N_{vars} \qquad (4.22)$$

The eigenvalues λ are found using the characteristic equation of the square matrix $J_f, det(A - \lambda I) = 0$. The Solution is conditionally stable if each eigenvalue satisfies the following test:

$$Re(\lambda_i) = |1 + h\lambda_i| \leq 1 \qquad (4.23)$$

The step size is chosen to be relatively small in the solution region where the curves display much variation and to be relatively large where the solution curves straightness out to approach lines with slope almost zero.[89] Before we attempt to adopt the step-size in solving the dynamic model by using method of lines, it is useful to compare the solutions obtained by both approaches. It is pointed out that RK4 and FD methods give almost identical results for all the key components and temperature as shown in Figure 4.2.

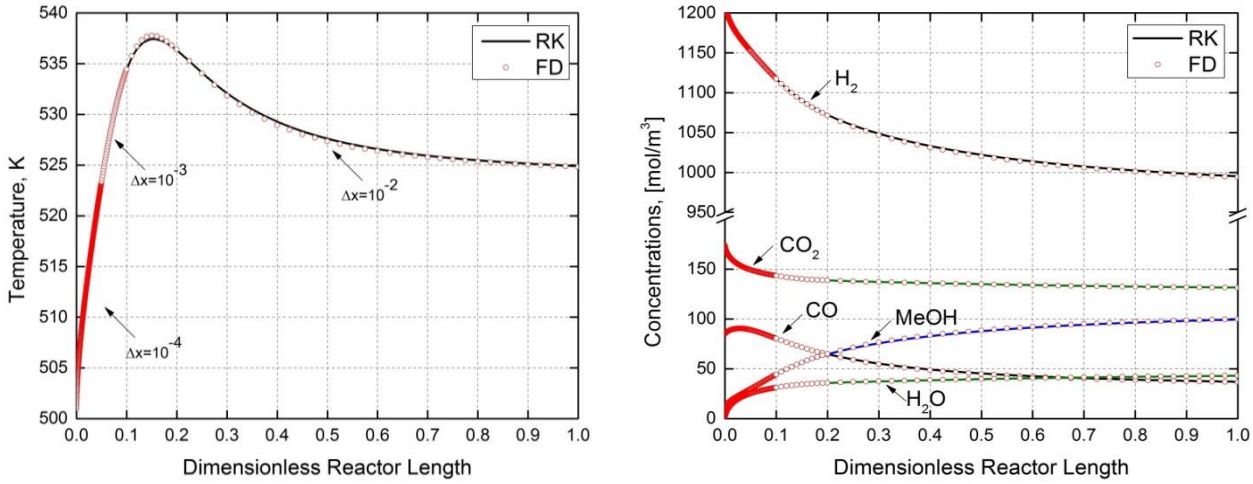

Figure 4.2: Temperature and concentrations profiles calculated by Runge-Kutta 4-th order and explicit finite difference methods.

Dynamic

As already mentioned earlier, the heterogeneous model of tubular reactor comprises approximately 15 partial differential and algebraic equations. The method of lines has been used for solving partial differential equations in which a forward finite difference method is used to

discretize the spatial domain with nearly 640 finite elements and then the resulting set of ODEs was numerically integrated through time. Dynamic simulator code developed using equations (4.7)-(4.18) accompanied with catalyst deactivation equations (4.19) and (4.20) in order to compute the reactor effluent and validate the mathematical model with the industrial data. Table 4.2 shows the predicated production rate of the reactor compared to the plant data over an operating time frame of about 1200 days. The dynamic simulation results match well with industrial data; therefore, we concurred that dynamic model with the proposed deactivation model parameters is reliable in predicting the reactor behavior.

Table 4.2: Comparison between plant data with the predicted methanol production.

Time (day)	Plant(ton/day)	Prediction(ton/day)	Error(%)
0	295	292	-1.01
100	296.5	286.6	-3.33
200	302.6	283.2	-6.41
300	284.3	280.6	-1.30
600	277.9	278.4	0.17
700	278.2	276.7	-0.53
800	253.0	275.0	8.69
900	274.0	273.4	-0.21
1000	268.1	272.1	1.49
1000	275.5	270.8	-1.70
1000	274.6	269.7	-1.78
1100	262.9	268.6	2.16
1200	255.2	267.6	4.85

Figure 4.3 shows the temperature profile and deactivation rate of catalyst with respect to the reactor length and the time horizon according to the dynamic stage simulation results. The catalyst activity drops to the lowest level (<0.5 at the end of run). Consequently, the maximum reactor temperature is 534 K at the start of run and gradually decreases over time.

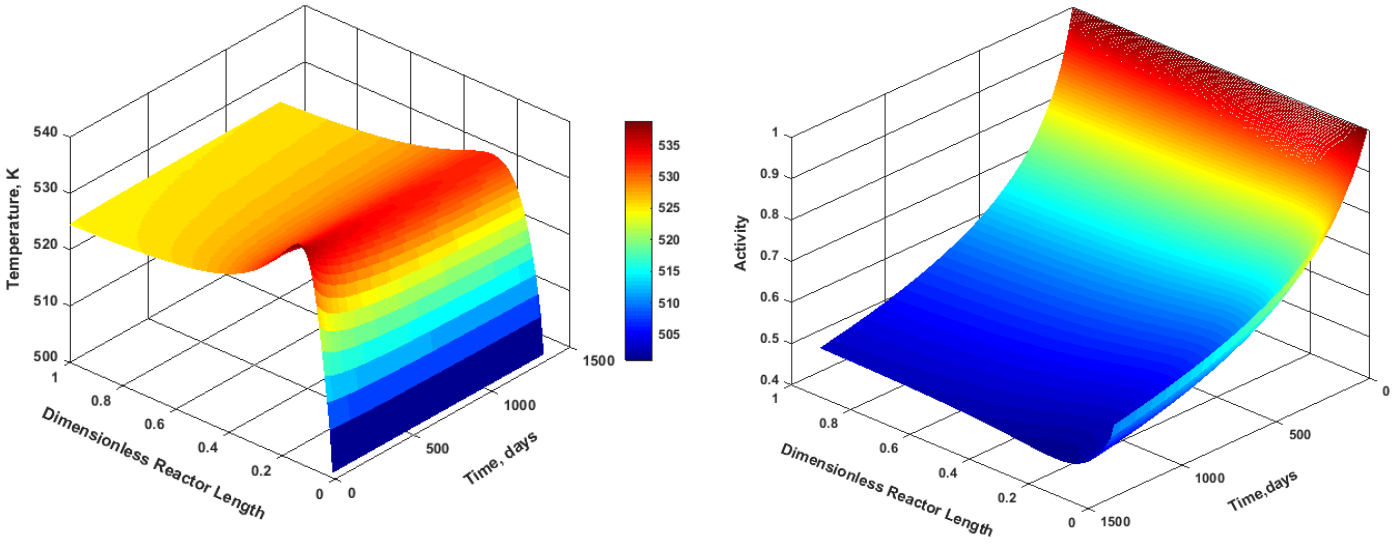

Figure 4.3: Temperature profile and catalyst activity.

Problem formulation

The task is finding the optimal operation strategy, namely shell coolant temperature trajectory and recycle ratio of CO_2 fed to the reactor. The objective was formulated as a nonlinear dynamic optimization problem:

$$max\left[J = \int_0^{t_f} Production(R_{Co2}, T_{shell}, t)dt\right] \quad (4.24)$$

Subject to:

$$0 \leq T \leq 543\ K \quad (4.25)$$

$$0 \leq R_{Co2} \leq 0.1 \quad (4.26)$$

$$490\ K \leq T_{shell} \leq 540\ K \quad (4.27)$$

The production rate function is obtained by solving the partial differential equations eq. (4.7) to (4.20).The shell coolant temperature is bounded between 490 and 540K and the recycle ratio of

CO_2 , defined as $R_{Co2} = F_{Co2}/F_{in}$, must be below or equal 0.1 as it is restricted by the plant's design flexibility. There is only one path constraint; the gas temperature along the reactor length must be below 543K to prevent severe deactivation rate. The objective function *J* is the value of the total methanol production over the catalyst lifetime period. The proposed hybrid algorithm was used for dynamic constrained optimization of the reactor operating conditions considering the above inequality constraints.

A hybrid Genetic - Generalized Pattern Search algorithm (GA-GPS) for the optimization problem

Genetic Algorithm (GA) is the most popular type of evolutionary algorithms that mimics the principle of biological evolution, repeatedly modifying a sample solution population using a technique inspired by natural evolution and uses random genetic operators such as mutation, selection and crossover.[90] GA is widely classified as a metaheuristic optimization algorithm due to its stochastic search mechanism which enables it to escape from local optima while exploring the search space for the global optimum in complex and rugged fitness landscapes.[91] In any metaheuristic algorithm, a compromise between exploration and exploitation components is carried out to balance the convergence rate of the algorithm and the likelihood of achieving the global optimality.[92,93] Exploration aims to generate diverse solutions by exploring a large solution space; whereas, exploitation narrows down the search to a specific regions with high-likelihood of containing a good solution. During the initialization step of GA, an initial population consisting of a number of individuals (NI) (each having a set of chromosomes or genotype (NG) to represent the decision variables for a particular solution), is randomly generated from the feasible search space. A fitness function is evaluated for each individual and then the population sorted by the

descending order of the fitness values. Subsequently, selection process considers only the fitness values regardless of the individuals' genotypes. Therefore, the selection is an exploitative operation since the mechanism does not care about the diversity of genotypes of each selected individuals but distinguishes them based on their fitness values. These selected individuals are used to perform the genetic operations: 1) mutating some individuals randomly replaces some of the existing genotypes with new ones; 2) crossover (exchanging a portion of genotype) is performed between two individuals (parents) to create two new individuals (children). Mutation and crossover are explorative operators because they introduce new genotypes to the population and spread the new generation over the search space with the hope of exploring new basins.[90] After enough generations, existing genotypes in the population become similar to each other and the mean fitness value of the populations becomes close to the best fitness value as illustrated in Figure 4.4.

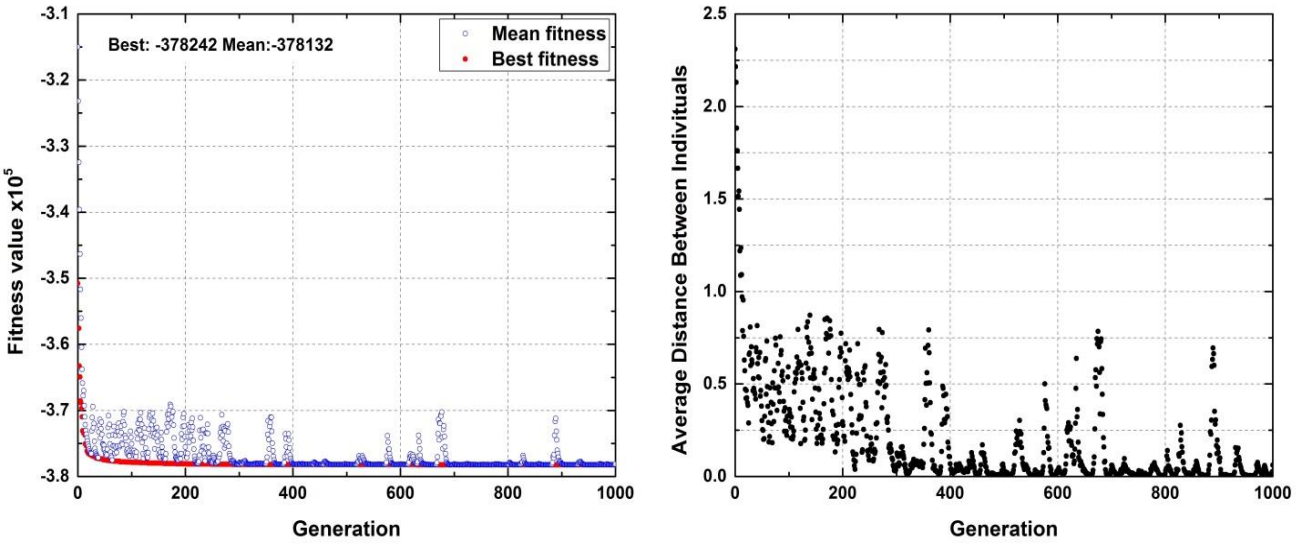

Figure 4.4: Best and mean fitness values and the average distance between individuals.

GA has been proven to be effective at escaping local optima and finding solutions closed to the global optimum/optima in even a very complex function. However, it shows weakness in efficiently exploiting the existing basins in order to find the optimal point.[94] Hence, it could be much efficient to use the output of GA as an input for a local search algorithm such as Generalized Pattern Search (GPS). GPS is a derivative-free optimization method that does not use the information about gradient or higher derivative to search for an optimal point.[95] Starting from an initial solution x_0 and an initial mesh size Δ_0^m=1, GPS generates a set of neighborhood points by multiplying the current mesh size by each pattern vector. These vectors are fixed-direction vectors and defined by the number of independent variables in the objective function, as in GPS, 2N vectors consisting of N positive and N negative vectors. In k iterations, GPS algorithm polls all the mesh points by computing their objective function values in order to find an improved point. If the polling step fails to find an improved point then the mesh size will be reduced by half $\Delta_{i+1}^{m} = 0.5\,\Delta_{i}^{m}$ and the current point is used for the next iteration k+1. Otherwise when a successful pooling takes place and an improved point is found, then the mesh size will be doubled $\Delta_{i+1}^{m} = 2\ \Delta_{i}^{m}$ and the current point is updated by the improved point for the next iteration as shown in Figure 4.5.

The incorporation of a local search algorithm like GPS is a good strategy for improving the accuracy of the approximate solution previously provided by the genetic algorithm. Thus, an appropriate sequential hybridization of GA and GPS can improve the exploitation of the basin of solution that was already explored by GA and can lead to find, as accurately as possible, a local optimum. To maximize methanol production, we implemented such a GA-GPS hybrid algorithm to problem of optimizing aforementioned reactor's operation conditions.

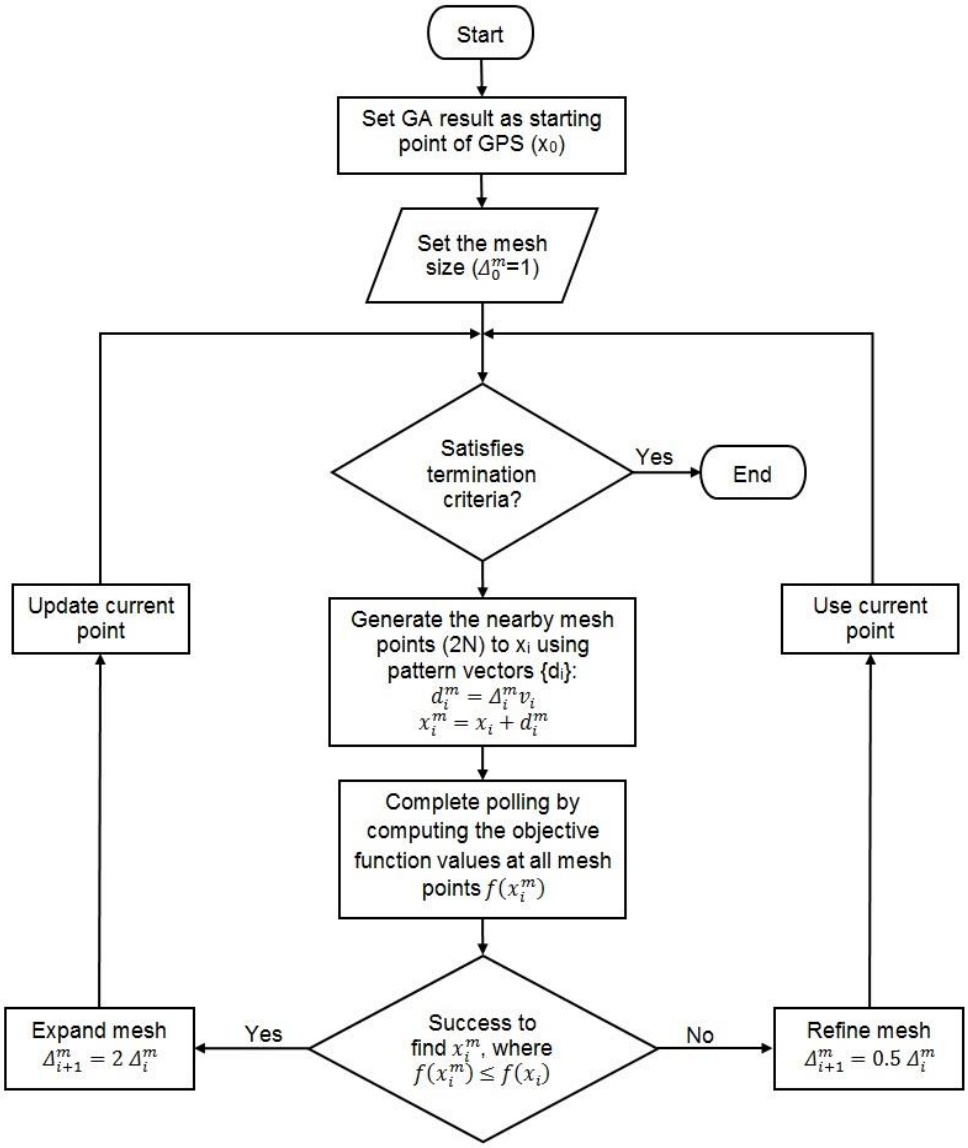

Figure 4.5: Flowchart of Hybrid GA-GPS Algorithm.

The first phase of GA-GPS hybrid algorithm is exploration via employing GA to minimize the fitness function, negative of the total production over the catalyst lifetime (-*J*). GA parameters were tuned by troubleshooting and the number of generations was set to 450. As indicated in Figure 4.4, the mean value of the fitness function is matched up to the best fitness value and no more diversity of individual. Each generation has a default population of 200 individuals and the

algorithm begins by creating a random initial population. These individuals are representing shell temperature and recycle ratio of CO_2 at each time segment. Then, the fitness value (score) of each individual are evaluated to select the best individuals for mutation and crossover processes. We used stochastic universal sampling (SUS) for the selection operation, where all individuals' scores are normalized and then mapped to adjoining segment of a line in such a way that each individual's segment is equal in size to its scores. SUS generates a single random value (specifying the starting point in [0, 1/Np] to sample all of the solutions by selecting an individual at every 1/Np distance where Np is the number of individuals to select. SUS shows no bias giving the low scored individuals a chance to be chosen. The next step is to generate the second generation of population by applying mutation and crossover on the selected individuals where 80% of the next population is produced by using GA's operators (crossover and mutation) and 20% elite individuals from the current and previous generations. The second phase involves an exploitative search employing GPS after receiving the best solution from GA and using it as an initial solution for GPS. A complete polling occurs by computing the objective function values at all mesh points $f(x_i^m)$ starting at the first iteration $(\Delta_0^m = 1)$ until some termination criteria are met (either $\Delta_i^m = 10^{-6}$ or 300 iterations).

RESULTS AND DISCUSSIONS

The time-horizon for the decision variables of the considered optimization problem, namely shell temperature and recycle ratio of CO_2, were discretized into sixteen intervals, i.e., each interval is a quarter of a year over the catalyst lifetime (four years). The optimization of reactor was investigated in two steps; dynamic stage optimization of shell temperature followed by simultaneous dynamic stag optimization of shell temperature and recycle ratio of CO_2.

Dynamic staged optimization of shell temperature

For this section, the ratio of recycled CO_2 directly fed to the reactor is set as 0%, 5%, and 10% of the total flow rate of the inlet stream; consequently equation (4.26) is ignored. Figure 4.6 shows the amount of methanol production rate associated with the approximately optimal shell temperature trajectories derived by the proposed GA-GPS algorithm. The proposed T_{shell} trajectory improved the associated production rates for 0%, 5%, and 10% recycle ratio of CO_2 by 1.67%, 2.53%, and 1.43%, respectively, compared to the reference case of keeping the shell temperature constantly at 524K. The optimal shell temperature trajectories for these cases gradually increase with time as expected to compensate for catalyst deactivation. In addition, the more CO_2 is fed to the system, the higher T_{sheel} is needed to supply more heat to the endothermic Reaction (4.6). Figure 4.6 shows that the optimal solution does not violate the path temperature constraint (4.27).

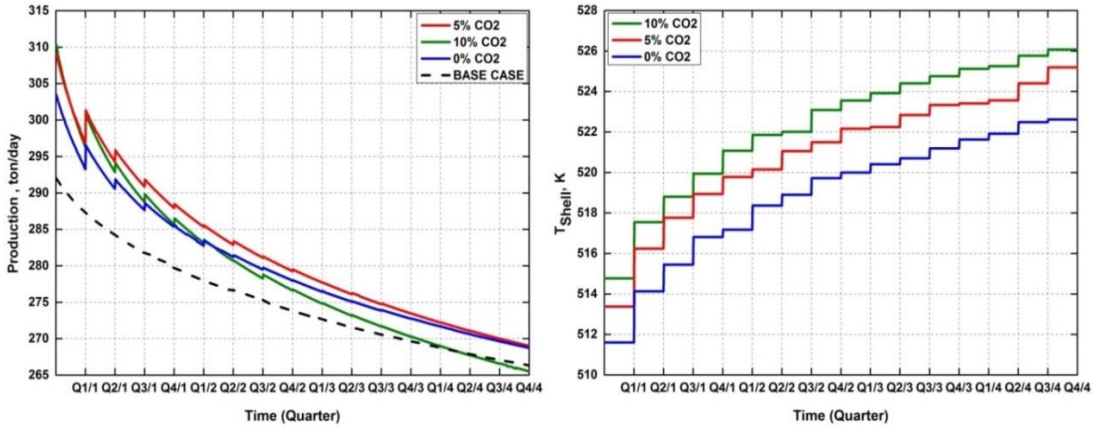

Figure 4.6: Predicted methanol production rate at different recycle ratio of CO2 ratio associated with the optimal shell temperature trajectory.

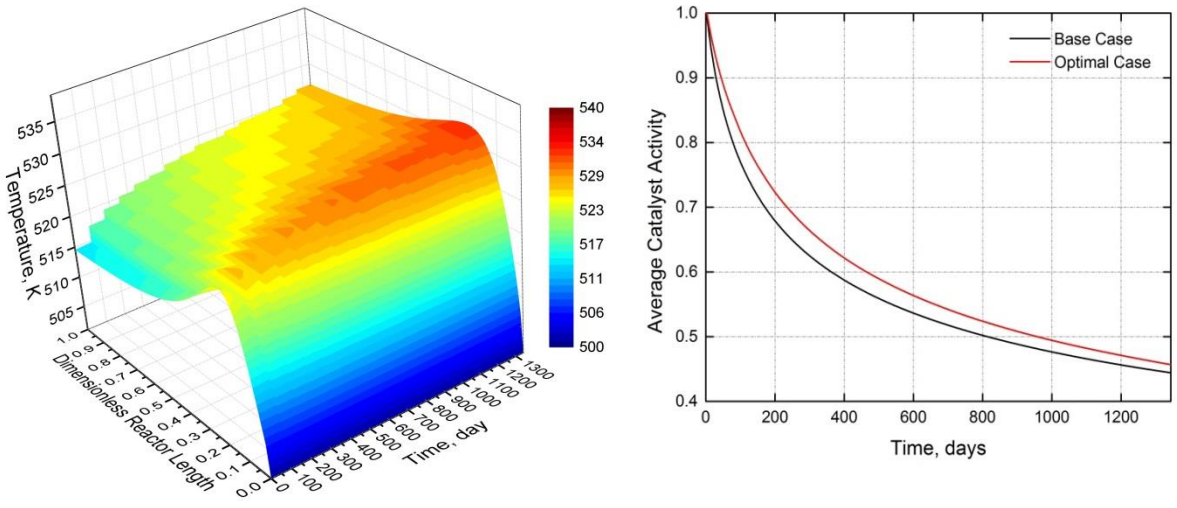

Figure 4.7: Reactor temperature and the average catalyst activity profiles at the optimal case (the optimal case: 5% recycle ratio of CO_2 and shell temperature trajectory shown in Figure 4.6).

The average catalyst activity versus time from both reference and optimal cases is shown in Figure 4.7. The average catalyst activity in the optimal case is higher than in the reference case as the reactor is operated at lower shell temperature during the whole lifetime cycle of the catalyst except the last two quarters.

Simultaneous dynamic stage optimization of shell temperature and recycle ratio of CO_2

For this section, we simultaneously optimized shell coolant temperature and recycle ratio of CO_2 to maximize the production rate. Figure 4.8 compares the production rates and T_{shell} trajectories for the proposed solution of the simultaneous optimization (referred to as 0-10% CO_2) with those for the proposed solution with fixed 5% recycle ratio of CO_2. As shown in Figure 4.8, the approximately optimal production rate for the 5% CO_2 and 0-10% CO_2 matches remarkably close.

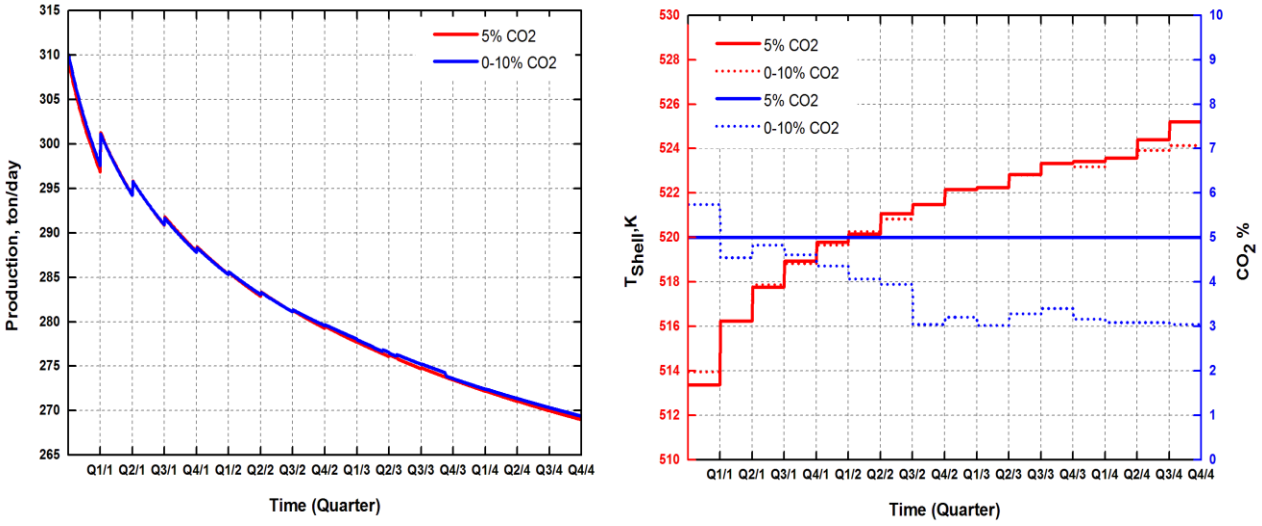

Figure 4.8: Predicted methanol production rates associated with the optimal shell temperature and recycle ratio of CO_2 trajectories.

This result implies that the recycle ratio of CO_2 can be kept at 5% over the decision horizon for operational simplicity without significantly reducing the production rate. This way, the number of variables can be reduced for this optimization problem from 32 to 16 by assuming a fixed amount of CO_2 is utilized (5%) to obtain the optimal production rate.

CONCLUSION

An industrial lurgi type methanol reactor with catalyst deactivation has been modeled and optimized with respect to the shell coolant temperature and the recycle ratio of CO_2 fed to the system. The results showed that correcting the syngas ratio of the inlet stream of the reactor system improves the production rate by increasing CO_2 recycled ratio to 5% of recovered CO_2 from the reformer flue gases. The production rates for 0% and 5% recycled CO_2 ratio cases were improved by 1.67% and 2.53%, respectively. These improvements are equivalent to 2.73 and 4.13 Million USD based on an average price of 400 per ton of methanol, respectively, over four years

of operation compared to the reference case (T_{shell} = 524K and no extra CO_2 added to the system). Since no tax is collected on fossil fuel production in the region where the plant is located (Middle East), this benefit calculation excluded the additional profit from avoiding/reducing the charge/tax for CO_2 emission into the atmosphere.

Chapter 5: CONCLUSIONS AND FUTURE WORK

This is an overall conclusion of the thesis, which is a summary of individual conclusions, given in each chapter.

In chapter 2, superconverter design has a capability to efficiently remove the heat generated by the exothermic reaction in methanol synthesis, and its temperature profile is very favorable, in terms of reaction rate and an increase in the production of methanol rate. The methanol mole fraction profile increases gradually and reaches 11.92% and 11.36% for the double tube exchanger and the conventional converter, respectively. Hence, the production of methanol is improved by 3%, compared to the conventional converter, while, at the same time, its operation is under mild conditions, especially at the end of the tube. This makes the catalyst lasts longer. This leads to process intensification and allows for the use of a compact distillation step. In addition, this new design has the advantage of preheating the feed gas in the reaction, and the inner tubes will replace the feed gas preheater.

In chapter 3, the multiobjective optimization problem of ICI's low pressure methanol process operating conditions has been performed for efficient methanol production with reduced CO_2 emission. To tackle this problem, the elitist non-dominated sorting genetic algorithm (NSGA-II) was adopted to determine the optimum amount of captured CO_2 that can be utilized, the favorable temperature, and the splitting factor of each quenching stream. The possibilities of improving the process were analyzed using a rigorous model integrated with a generic process flowsheet to obtain necessary comparative results. In contrast to the base case of an industrial plant, the results have illustrated different operating conditions to operate the plant at different carbon dioxide consumption levels and production rates. It is shown that the highest methanol generation by the

quench converter is ~2778 MTPD when ~5010 MTPD of carbon dioxide is consumed. This leads to an improvement in plant production of 3% and also prevents 3430 MTPD of CO_2 from being released to the atmosphere. The main advantage of applying multiobjective optimization is the ability to choose one of the optimal solutions based on a good knowledge of the process and the preferred condition.

In chapter 4, an industrial lurgi-type reactor with catalyst deactivation has been modeled and optimized with respect to coolant temperature and the recycle ratio of CO_2 fed to the system. A hybrid algorithm combining genetic algorithm (GA) and generalized pattern search (GPS) provides a sufficiently good solution and converges faster than GA alone. The results showed that correcting the SN of the inlet stream of the reactor system improves the production rate by increasing the CO2 recycled ratio to 5% of recovered CO_2 from the reformer flue gases. The production rates for 0% and 5% recycled CO_2 ratio cases were improved by 1.67% and 2.53%, respectively. These improvements are equivalent to 2.73 and 4.13 million USD based on an average price of 400 USD per ton of methanol, respectively, over four years of operation compared to the reference case.

The main contribution of this thesis is modeling and optimization of methanol synthesis from syngas in the gas phase and consideration of the most commercially matured methanol synthesis technologies. A rigorous model is used to demonstrate the superiority of the new double-tube reactor, which was developed through cooperation between Mitsubishi Heavy Industries, Ltd (MHI) and Mitsubishi Gas Chemical Co., Inc. (MGC), with respect to high efficiency and less energy consumption. To the best of our knowledge, this is the first work that shows how this reactor type has a higher production rate than a conventional single-tube reactor by more than 3%,

so that a compact purification step can be used. It also shows that preheating the feed gas inside the inner tubes replaces the feed gas preheater.

This thesis also carried out a steady-state multi-objective optimization of ICI's low pressure methanol process utilized adiabatic quench-type reactor. A non-dominated genetic algorithm (NSGA-II) was adopted to determine the optimum amount of captured CO_2 that can be utilized, the favorable temperature and the splitting factor of each quenching stream. A Hybrid GA-GPS optimization algorithm was applied on an industrial lurgi-type methanol reactor with catalyst deactivation to accurately and rapidly find the optimal shell coolant temperature trajectory and the recycle ratio of CO_2.

FUTURE WORK

One of the key success factors for methanol producers is cost control of the methanol production process to ensure maximum profit. Methanol costs are mainly driven by feedstock cost and capital cost. Producers usually secure long term contracts for supplying natural gas at a certain fixed cost. Hence, producing methanol in mega-scale (>3000 MTPD) becomes essential to have an opportunity to compete in the market. In parallel with the shale gas boom due to new technology in hydraulic fracturing, the world leaders (MHI and Lurgi) in methanol synthesis process technologies have developed and thoroughly implemented mega-scale methanol plants across the world. An autothermal reformer is implemented in both technologies to reduce the overall capital cost of the plant as well as to achieve a favorable syngas ratio. Although the results presented herein have demonstrated the effectiveness of these technologies and performed some derivative-

free optimization techniques into process schemes, there is room for further development in a number of ways:

1. Integrating the methanol synthesis process with ATR synthesis gas technology.
2. Extending the optimization algorithms to work on mega-scale plants including the syngas production step to achieve high efficiencies, ensuring reduction in energy and meet environmental regulations.
3. Finding the optimal operation including the amount of flue gas recycled to the ATR and/or methanol synthesis loop.

PUBLICATIONS

1. Alarifi, Abdulaziz, Ali Elkamel, and Eric Croiset. "Steady-State Simulation of a Novel Annular Multitubular Reactor for Enhanced Methanol Production."*Industrial & Engineering Chemistry Research* 52, no. 44 (2013): 15387-15393.
2. Alarifi, Abdulaziz, Saad Alsobhi, Ali Elkamel, and Eric Croiset. "Multiobjective Optimization of Methanol Synthesis Loop from Synthesis Gas via a Multibed Adiabatic Reactor with Additional Interstage CO2 Quenching." *Energy & Fuels* 29, no. 2 (2015): 530-537.
3. Alarifi, Abdulaziz, Zhefu Liu, Fatih Erenay, Ali Elkamel, and Eric Croiset. "Dynamic Optimization of Lurgi Type Methanol Reactor Using Hybrid GA-GPS Algorithm: Optimal Shell Temperature Trajectory and Carbon Dioxide Utilization." *Industrial & Engineering Chemistry Research.*

REFERENCES

(1) Olah, George A., Alain Goeppert, and GK Surya Prakash. "Chemical recycling of carbon dioxide to methanol and dimethyl ether: from greenhouse gas to renewable, environmentally carbon neutral fuels and synthetic hydrocarbons." *The Journal of organic chemistry* 74.2 (2008): 487-498.

(2) Olah, George A. "Beyond oil and gas: the methanol economy." Angewandte Chemie *International Edition* 44, no. 18 (2005): 2636-2639.

(3) Olah, George A., and GK Surya Prakash. "Efficient and selective conversion of carbon dioxide to methanol, dimethyl ether and derived products." U.S. Patent 7,605,293, issued October 20, 2009.

(4) Machiele, Paul A. Summary of the Fire Safety Impacts of Methanol as a Transportation fuel. No. 901113. *SAE Technical Paper*, 1990.

(5) Alarifi, Abdulaziz, Saad Alsobhi, Ali Elkamel, and Eric Croiset. "Multiobjective Optimization of Methanol Synthesis Loop from Synthesis Gas via a Multibed Adiabatic Reactor with Additional Interstage CO2 Quenching." *Energy & Fuels*29, no. 2 (2015): 530-537.

(6) Grube, Thomas. *Methanol as an energy carrier*. Edited by Peter Biedermann. Forschungszentrum, Zentralbibliothek, 2006.

(7) Lee, Sunggyu. *Methanol synthesis technology*. CRC Press, 1989.

(8) Arthur, Theophilus. "Control structure design for methanol process."*Department of Chemical Engineering, Norwegian University of Science and Technology, Trondheim* (2010): 1-91.

(9) Hotchkiss, R. "Coal gasification technologies." *Proceedings of the Institution of Mechanical Engineers, Part A: Journal of Power and Energy* 217, no. 1 (2003): 27-33.

(10) "Methanol plant design choices affect operations, costs, other equipment." *Oil & Gas Journal (1993)*.53.

(11) Ramos, Leonardo, and Susana Zeppieri. "Feasibility study for mega plant construction of synthesis gas to produce ammonia and methanol." *Fuel* 110 (2013): 141-152.

(12) Natta, G. "Synthesis of methanol." *Catalysis* 3 (1955): 349-411.

(13) Bakemeier, Heinrich, Peter R. Laurer, and Wolfgang Schroder. "Development and application of a mathematical model of the methanol synthesis." *Chem. Eng. Prog.;(United States)* 66, no. 98 (1970).

(14) Leonov, V. E., M. M. Karavaev, E. N. Tsybina, and G. S. Petrishcheva. "Kinetics of methanol synthesis on a low-temperature catalyst." *Kinet. Katal* 14 (1973): 970-975.

(15) Herman, R. G., K. Klier, G. W. Simmons, B. P. Finn, Jl B. Bulko, and T. P. Kobylinski. "Catalytic synthesis of methanol from COH2: I. Phase composition, electronic properties, and activities of the Cu/ZnO/M2O3 catalysts." *Journal of Catalysis* 56, no. 3 (1979): 407-429.

(16) Klier, K., V. Chatikavanij, R. G. Herman, and G. W. Simmons. "Catalytic synthesis of methanol from COH2: IV. The effects of carbon dioxide." *Journal of Catalysis* 74, no. 2 (1982): 343-360.
(17) Graaf, G. H., E. J. Stamhuis, and A. A. C. M. Beenackers. "Kinetics of low-pressure methanol synthesis." *Chemical Engineering Science* 43, no. 12 (1988): 3185-3195.
(18) McNeil, Melanie A., Carl J. Schack, and Robert G. Rinker. "Methanol synthesis from hydrogen, carbon monoxide and carbon dioxide over a CuO/ZnO/Al2O3 catalyst: II. Development of a phenomenological rate expression." *Applied catalysis* 50, no. 1 (1989): 265-285.
(19) Bussche, KM Vanden, and G. F. Froment. "A steady-state kinetic model for methanol synthesis and the water gas shift reaction on a commercial Cu/ZnO/Al2O3 catalyst." *Journal of Catalysis* 161, no. 1 (1996): 1-10.
(20) ChemSystems, Nexant. " Methanol " *Nexant Report:* (2008).
(21) Al-Fadli, A.M Soliman, M.A , Froment, G. . "Steady State Simulation of a Multi-Bed Adiabatic Reactor for Methanol Production. "*J. King Saud Univ*, no. 7(1995): 101-133.
(22) Matsumoto, Hiroshi, H. Nagai, Haruhito Watanabe, K. Morita, and H. Makihara. "Advanced technology for large scale methanol plant." *Mitsubishi Heavy Industries Technical Review* 34, no. 2 (1997): 58-62.
(23) Bromberg, L., and W. K. Cheng. "Methanol as an alternative transportation fuel in the US: Options for sustainable and/or energy-secure transportation."*Cambridge, MA: Sloan Automotive Laboratory, Massachusetts Institute of Technology* (2010).
(24) "Chalmers looks to replace hydrogen with methanol as future fuel." *Fuel Cells Bull.* (2012):9−10.
(25) Olah, George A., Alain Goeppert, and GK Surya Prakash. *Beyond oil and gas: the methanol economy*. John Wiley & Sons, 2011.
(26) Tijm, P. J. A., F. J. Waller, and D. M. Brown. "Methanol technology developments for the new millennium." *Applied Catalysis A: General* 221, no. 1 (2001): 275-282.
(27) Kobayashi, Kazuto, Hiroyuki Osora, Hideaki Nagai, and Hiroshi Ohira. "Apparatus for methanol synthesis." U.S. Patent 7,189,379, issued March 13, 2007.
(28) Bakemeier, Heinrich. *Methanol technology and economics*. Vol. 66. American Institute of Chemical Engineers, 1970.
(29) Villa, Pierluigi, Pio Forzatti, Guido Buzzi-Ferraris, Guido Garone, and Italo Pasquon. "Synthesis of alcohols from carbon oxides and hydrogen. 1. Kinetics of the low-pressure methanol synthesis." *Industrial & engineering chemistry process design and development* 24, no. 1 (1985): 12-19.
(30) Graaf, G. H., H. Scholtens, E. J. Stamhuis, and A. A. C. M. Beenackers. "Intra-particle diffusion limitations in low-pressure methanol synthesis."*Chemical Engineering Science* 45, no. 4 (1990): 773-783.

(31) Graaf, G. H., P. J. J. M. Sijtsema, E. J. Stamhuis, and G. E. H. Joosten. "Chemical equilibria in methanol synthesis." *Chemical Engineering Science* 41, no. 11 (1986): 2883-2890.
(32) Malinovskaya, O. A., A. Ya Rozovskii, I. A. Zolotarskii, Yu V. Lender, Yu Sh Matros, G. I. Lin, G. V. Dubovich, N. A. Popova, and N. V. Savostina. "Synthesis of methanol on Cu-based catalyst: Kinetic model." *Reaction Kinetics and Catalysis Letters* 34, no. 1 (1987): 87-92.
(33) Chinchen, G. C., P. J. Denny, D. G. Parker, M. S. Spencer, and D. A. Whan. "Mechanism of methanol synthesis from CO 2/CO/H 2 mixtures over copper/zinc oxide/alumina catalysts: use of 14 C-labelled reactants." *Applied Catalysis* 30, no. 2 (1987): 333-338.
(34) Chinchen, G. C., P. J. Denny, J. R. Jennings, M. S. Spencer, and K. C. Waugh. "Synthesis of methanol: part 1. Catalysts and kinetics." *Applied Catalysis* 36 (1988): 1-65.
(35) Muhler, Martin, Eric Törnqvist, Lars P. Nielsen, Bjerne S. Clausen, and Henrik Topsøe. "On the role of adsorbed atomic oxygen and CO2 in copper based methanol synthesis catalysts." *Catalysis letters* 25, no. 1-2 (1994): 1-10.
(36) Froment, Gilbert F., Kenneth B. Bischoff, and Juray De Wilde. *Chemical reactor analysis and design*. Vol. 2. New York: Wiley, 1990.
(37) Reid, Robert C., John M. Prausnitz, and Bruce E. Poling. "The properties of gases and liquids." (1987).
(38) Fuller, E. N., and J. C. Giddings. "A comparison of methods for predicting gaseous diffusion coefficients." *Journal of Chromatographic Science* 3, no. 7 (1965): 222-227.
(39) Fuller, Edward N., Paul D. Schettler, and J. Calvin Giddings. "New method for prediction of binary gas-phase diffusion coefficients." *Industrial & Engineering Chemistry* 58, no. 5 (1966): 18-27.
(40) Fuller, Edward N., Keith Ensley, and J. Calvin Giddings. "Diffusion of halogenated hydrocarbons in helium. The effect of structure on collision cross sections." *The Journal of Physical Chemistry* 73, no. 11 (1969): 3679-3685.
(41) Cussler, Edward Lansing. *Diffusion: mass transfer in fluid systems*. Cambridge university press, 2009.
(42) Koning, Gijsbertus Wilhelmus. *Heat and mass transport in tubular packed bed reactors at reacting and non-reacting conditions: experiments and models*. Twente University Press, 2002.
(43) Dixon, Anthony G. "An improved equation for the overall heat transfer coefficient in packed beds." *Chemical Engineering and Processing: Process Intensification* 35, no. 5 (1996): 323-331.
(44) Dixon, Anthony G., and David L. Cresswell. "Theoretical prediction of effective heat transfer parameters in packed beds." *AIChE Journal* 25, no. 4 (1979): 663-676.
(45) Dixon, Anthony G. "Wall and particle-shape effects on heat transfer in packed beds." *Chemical engineering communications* 71, no. 1 (1988): 217-237.

(46) Makihara, H., K. Niwa, H. Nagai, K. Morita, H. Horizoe, K. Kobayashi, and C. Kuwada. "Characteristics of a new methanol synthesis reactor." *Energy progress* 7, no. 1 (1987): 51-58.
(47) Olah, George A., and GK Surya Prakash. "hydrogenatively converting the carbon dioxide into methanol; use as fuel, or to reduce the risk of transporting hydrogen, liquid natural gas fuels; carbon neutral." U.S. Patent 8,212,088, issued July 3, 2012.
(48) Methanol Fuels and Fire Safety , Fact Sheet OMS-8 (Washington, DC, 1994), http://www.epa.gov/otaq/consumer/08-fire.pdf.
(49) Chapel, Dan G., Carl L. Mariz, and John Ernest. "Recovery of CO2 from flue gases: commercial trends." In *Canadian Society of Chemical Engineers Annual Meeting*, pp. 4-6. 1999.
(50) Cheng, Wh-Hsun, ed. *Methanol production and use*. CRC Press, 1994.
(51) Al-Fadli, A. M., M. A. Soliman, and G. F. Froment. "Simulation of transients in a multi bed adiabatic methanol synthesis reactor." In *fourth saudi engineering conference, Riyadh, Saudi Arabia*, pp. 121-127. 1995.
(52) Beckett, P. C., T. I. Evans, W. E. Ryan, and A. Akgerman. "Designing a multistage adiabatic reactor for minimum catalyst volume." *Chemical Engineering Communications* 76, no. 1 (1989): 107-124.
(53) Lange, Jean-Paul. "Methanol synthesis: a short review of technology improvements." *Catalysis Today* 64, no. 1 (2001): 3-8.
(54) Liu, Pei, Dimitrios I. Gerogiorgis, and Efstratios N. Pistikopoulos. "Modeling and optimization of polygeneration energy systems." *Catalysis Today* 127, no. 1 (2007): 347-359.
(55) Julián-Durán, Laura M., Andrea P. Ortiz-Espinoza, Mahmoud M. El-Halwagi, and Arturo Jiménez-Gutiérrez. "Techno-economic assessment and environmental impact of shale gas alternatives to methanol." *ACS Sustainable Chemistry & Engineering* 2, no. 10 (2014): 2338-2344.
(56) Alarifi, Abdulaziz, Ali Elkamel, and Eric Croiset. "Steady-State Simulation of a Novel Annular Multitubular Reactor for Enhanced Methanol Production."*Industrial & Engineering Chemistry Research* 52, no. 44 (2013): 15387-15393.
(57) Zahedi, G., A. Elkamel, and A. Lohi. "Enhancing CO2 conversion to methanol using dynamic optimization, applied on shell temperature and inlet hydrogen during four years operation of methanol plant." *Energy Sources, Part A* 29, no. 15 (2007): 1385-1396.
(58) Zahedi, G., A. Elkamel, and A. Lohi. "Dynamic optimization strategies of a heterogeneous reactor for CO2 conversion to methanol." *Energy & Fuels* 21, no. 5 (2007): 2977-2983.
(59) Løvik, Ingvild. "Modelling, estimation and optimization of the methanol synthesis with catalyst deactivation." (2001).
(60) Plus, Aspen. "User Guide Version 10.2." *Aspen Technology Inc., Cambridge, USA* (2000).
(61) Toolbox, Global Optimization. "User's Guide (r2011b)." *The MathWorks, September* (2011).

(62) Deb, Kalyanmoy. *Multi-objective optimization using evolutionary algorithms*. Vol. 16. John Wiley & Sons, 2001.
(63) Nandasana, Anjana D., Ajay Kumar Ray, and Santosh K. Gupta. "Applications of the non-dominated sorting genetic algorithm (NSGA) in chemical reaction engineering." *International journal of chemical reactor engineering* 1 (2003): No-pp.
(64) Ilyukhin, N. A.; Mikhailov, A. "Collaboration between JSC "Metafrax" and "Methanol Casale S.A." for Revamping Methanol Production Plant". *In Casale 3rd Customer Symposium, Lugano, Switzerland*, 2011.
(65) Herdem, Münür Sacit, Siamak Farhad, Ibrahim Dincer, and Feridun Hamdullahpur. "Thermodynamic modeling and assessment of a combined coal gasification and alkaline water electrolysis system for hydrogen production."*International Journal of Hydrogen Energy* 39, no. 7 (2014): 3061-3071.
(66) Aresta, M., and I. Tommasi. "Carbon dioxide utilisation in the chemical industry." *Energy conversion and management* 38 (1997): S373-S378.
(67) Gunardson, Harold H., ed. *Industrial gases in petrochemical processing: chemical industries*. CRC Press, 1997.
(68) Beychok, M. Fossil Fuel Combustion Flue Gases. *eoearth.org*.
(69) Metz, Bert, Ogunlade Davidson, Heleen de Coninck, Manuela Loos, and Leo Meyer. "Carbon dioxide capture and storage." (2005).
(70) Treacy, Damien, and Julian RH Ross. "The potential of the CO2 reforming of CH4 as a method of CO2 mitigation. A thermodynamic study." *Prepr. Pap.-Am. Chem. Soc., Div. Fuel Chem* 49, no. 1 (2004): 127.
(71) Halmann, Martin M. *Chemical Fixation of Carbon Dioxide Methods for Recycling CO2 into Useful Products*. CRC press, 1993.
(72) Suib, Steven L., ed. *New and Future Developments in Catalysis: Activation of Carbon Dioxide*. Newnes, 2013.
(73) Jessop, Philip G. "Greenhouse Gas Carbon Dioxide Mitigation: Science and Technology By Martin M. Halmann (Weizmann Institute of Science, Israel) and Meyer Steinberg (Brookhaven National Laboratory). Lewis Publishers: Boca Raton, FL. 1999. xix+ 568 pp. $99.95. ISBN 1-56670-284-4." *Journal of the American Chemical Society* 123, no. 29 (2001): 7197-7197.
(74) Halmann, Martin M., and Meyer Steinberg. *Greenhouse gas carbon dioxide mitigation: science and technology*. CRC press, 1998.
(75) ST. C., TEUNER, P. Neumann, and F. Von Linde. "The calcor standard and calcor economy processes." *Oil Gas European Magazine* (2001): 45.
(76) Kurz, German, and Stefan Teuner. "Calcor process for CO production." *Erdöl und Kohle, Erdgas, Petrochemie* 43, no. 5 (1990): 171-172.
(77) Shi, Fan, ed. *Reactor and Process Design in Sustainable Energy Technology*. Elsevier, 2014.

(78) Zittel, Werner, and Reinhold Wurster. "Hydrogen in the energy sector." *Ludwig-Bölkow-Systemtechnik GmbH* (1996).
(79) Badwal, Sukhvinder PS, Sarbjit S. Giddey, Christopher Munnings, Anand I. Bhatt, and Anthony F. Hollenkamp. "Emerging electrochemical energy conversion and storage technologies." *Frontiers in chemistry* 2 (2014).
(80) Reddy, Satish, Mukund Bhakta, John Gilmartin, and Joseph Yonkoski. "Cost Effective CO 2 Capture from Flue Gas for Increasing Methanol Plant Production." *Energy Procedia* 63 (2014): 1407-1414.
(81) FILIPPI, E. PROCESS FOR PRODUCING METHANOL FROM STEAM REFORMING. WO Pat. 2,009,127,657 2009.
(82) SPC. Methanol Reactor Long Sheet; Shiraz Petrochemical Company, 2000–2003.
(83) Koning, B. Heat and Mass Transport in Tubular Packed Bed Reactors at Reacting and Non-Reacting Conditions, University of Twente, 2002.
(84) Forzatti, Pio, and Luca Lietti. "Catalyst deactivation." Catalysis today 52, no. 2 (1999): 165-181.
(85) Løvik, Ingvild, Magne Hillestad, and Terje Hertzberg. "Modeling and optimization of a reactor system with deactivating catalyst." Computers & Chemical Engineering 23 (1999): S839-S842.
(86) Hanken, Linda. "Optimization of methanol reactor." *Master's thesis, The Norwegian University of Science and Technology* (1995).
(87) Hartman, Philip. "Ordinary differential equations." (1964).
(88) Heath, M. T. "Scientific Computing- An Introductory Survey. McGraw-Hill: New York, 1997."
(89) Liu, Shean-Lin. "Stable explicit difference approximations to parabolic partial differential equations." AIChE Journal 15, no. 3 (1969): 334-338.
(90) Golberg, David E. "Genetic algorithms in search, optimization, and machine learning." *Addion wesley* 1989 (1989).
(91) Bajpai, Pratibha, and Manoj Kumar. "Genetic algorithm–an approach to solve global optimization problems." *Indian Journal of computer science and engineering* 1, no. 3 (2010): 199-206.
(92) John Henry Holland. *Adaptation in natural and artificial systems: an introductory analysis with applications to biology, control, and artificial intelligence*. MIT press, 1992.
(93) Blum, Christian, and Andrea Roli. "Metaheuristics in combinatorial optimization: Overview and conceptual comparison." *ACM Computing Surveys (CSUR)* 35, no. 3 (2003): 268-308.
(94) Preux, Ph, and E-G. Talbi. "Towards hybrid evolutionary algorithms."*International transactions in operational research* 6, no. 6 (1999): 557-570.
(95) Rios, Luis Miguel. *Algorithms for derivative-free optimization*. ProQuest, 2009.

Appendix A

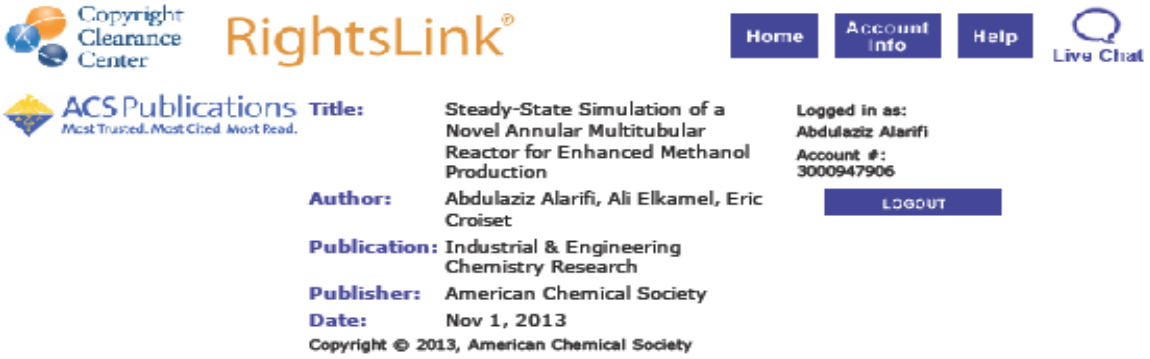

PERMISSION/LICENSE IS GRANTED FOR YOUR ORDER AT NO CHARGE

This type of permission/license, instead of the standard Terms & Conditions, is sent to you because no fee is being charged for your order. Please note the following:

- Permission is granted for your request in both print and electronic formats, and translations.
- If figures and/or tables were requested, they may be adapted or used in part.
- Please print this page for your records and send a copy of it to your publisher/graduate school.
- Appropriate credit for the requested material should be given as follows: "Reprinted (adapted) with permission from (COMPLETE REFERENCE CITATION). Copyright (YEAR) American Chemical Society." Insert appropriate information in place of the capitalized words.
- One-time permission is granted only for the use specified in your request. No additional uses are granted (such as derivative works or other editions). For any other uses, please submit a new request.

BACK CLOSE WINDOW

Copyright © 2015 Copyright Clearance Center, Inc. All Rights Reserved. Privacy statement. Terms and Conditions.
Comments? We would like to hear from you. E-mail us at customercare@copyright.com

Copyright Clearance Center RightsLink®

Home | Account Info | Help | Live Chat

ACS Publications Most Trusted. Most Cited. Most Read.

Title: Multiobjective Optimization of Methanol Synthesis Loop from Synthesis Gas via a Multibed Adiabatic Reactor with Additional Interstage CO2 Quenching

Author: Abdulaziz Alarifi, Saad Alsobhi, Ali Elkamel, et al

Publication: Energy & Fuels

Publisher: American Chemical Society

Date: Feb 1, 2015

Copyright © 2015, American Chemical Society

Logged in as: Abdulaziz Alarifi
Account #: 3000947906
LOGOUT

PERMISSION/LICENSE IS GRANTED FOR YOUR ORDER AT NO CHARGE

This type of permission/license, instead of the standard Terms & Conditions, is sent to you because no fee is being charged for your order. Please note the following:

- Permission is granted for your request in both print and electronic formats, and translations.
- If figures and/or tables were requested, they may be adapted or used in part.
- Please print this page for your records and send a copy of it to your publisher/graduate school.
- Appropriate credit for the requested material should be given as follows: "Reprinted (adapted) with permission from (COMPLETE REFERENCE CITATION). Copyright (YEAR) American Chemical Society." Insert appropriate information in place of the capitalized words.
- One-time permission is granted only for the use specified in your request. No additional uses are granted (such as derivative works or other editions). For any other uses, please submit a new request.

BACK | CLOSE WINDOW

Copyright © 2015 Copyright Clearance Center, Inc. All Rights Reserved. Privacy statement. Terms and Conditions.
Comments? We would like to hear from you. E-mail us at customercare@copyright.com

Copyright Clearance Center RightsLink®

Home | Create Account | Help | Live Chat

ACS Publications
Most Trusted. Most Cited. Most Read.

Title: Dynamic Optimization of Lurgi Type Methanol Reactor Using Hybrid GA-GPS Algorithm: Optimal Shell Temperature Trajectory and Carbon Dioxide Utilization

Author: abdulaziz alarifi, Zhefu Liu, Fatih Erenay, et al

Publication: Industrial & Engineering Chemistry Research

Publisher: American Chemical Society

Date: Dec 1, 2015

Copyright © 2015, American Chemical Society

LOGIN

If you're a copyright.com user, you can login to RightsLink using your copyright.com credentials. Already **a RightsLink user** or want to learn more?

PERMISSION/LICENSE IS GRANTED FOR YOUR ORDER AT NO CHARGE

This type of permission/license, instead of the standard Terms & Conditions, is sent to you because no fee is being charged for your order. Please note the following:

- Permission is granted for your request in both print and electronic formats, and translations.
- If figures and/or tables were requested, they may be adapted or used in part.
- Please print this page for your records and send a copy of it to your publisher/graduate school.
- Appropriate credit for the requested material should be given as follows: "Reprinted (adapted) with permission from (COMPLETE REFERENCE CITATION). Copyright (YEAR) American Chemical Society." Insert appropriate information in place of the capitalized words.
- One-time permission is granted only for the use specified in your request. No additional uses are granted (such as derivative works or other editions). For any other uses, please submit a new request.

BACK | CLOSE WINDOW

Copyright © 2016 Copyright Clearance Center, Inc. All Rights Reserved. Privacy statement. Terms and Conditions.
Comments? We would like to hear from you. E-mail us at customercare@copyright.com